Contrib Mineral Petrol (2007) 153:669–687
DOI 10.1007/s00410-006-0169-1

ORIGINAL PAPER

Intraplate volcanism in New Zealand: the role of fossil plume material and variable lithospheric properties

Peter Sprung · Stephan Schuth · Carsten Münker · Leonore Hoke

Received: 14 July 2006 / Accepted: 23 November 2006 / Published online: 6 January 2007

Abstract The geologic evolution of the New Zealand microcontinent was characterised by intermittent Cretaceous to Quaternary episodes of intraplate volcanism. To evaluate the corresponding mantle evolution beneath New Zealand with a specific focus on the tectonic evolution, we performed a combined major and trace element and Hf, Nd, Pb, Sr isotope investigation on a suite of representative intraplate volcanic rocks from both main islands and the Chatham Islands. Isotopically, the data set covers a range between ''HIMU-like'' end member compositions ($^{206}Pb/^{204}Pb$: 20.57, $^{207}Pb/^{204}Pb$: 15.77, $^{87}Sr/^{86}Sr$: 0.7030, εHf: + 3.8, εNd: + 4.2), compositions tending towards MORB ($^{206}Pb/^{204}Pb$: 19.01, $^{207}Pb/^{204}Pb$: 15.62, $^{87}Sr/^{86}Sr$: 0.7028, εHf: + 9.9, εNd: + 7.0) and compositions reflecting the influence of subducted sediments ($^{206}Pb/^{204}Pb$: 18.99, $^{207}Pb/^{204}Pb$: 15.67, $^{87}Sr/^{86}Sr$: 0.7037, εHf: + 4.4, εNd: + 3.9). Whereas volcanism on the Chatham Islands constitutes the HIMU end member of our data set, intraplate volcanic rocks from the North Island are dominated by MORB-like compositions with relatively radiogenic $^{206}Pb/^{204}Pb$ signatures. Volcanic rocks from the South Island form a trend between the three end members. Assuming a polybaric melting column model, the primary melt compositions reflect variations in the degree of melting, coupled to variable average melting depths. As the three isotope and trace element end members occur throughout the volcanic episodes, the ''HIMU-like'' and the sediment influenced signatures most likely originate from a heterogeneous subcontinental lithospheric mantle, whereas an asthenospheric origin is inferred for the MORB-like component. For the South Island, affinities to HIMU wane with decreasing average melting depths whereas MORB and sediment-like signatures become more distinct. We therefore propose a polybaric melting model involving upper asthenospheric mantle and a lithospheric mantle source that has been modified by subduction components and veins of fossil ''HIMU-like'' asthenospheric melts. The proportion of asthenospheric versus lithospheric source components is controlled by variations in lithospheric thickness and heat flow, reflecting the different tectonic settings and rates of extension. Generally, low degree melts preferentially tap enriched vein material with HIMU signatures. The widespread occurrence of old Gondwana-derived lithospheric mantle beneath intraplate volcanic fields in East Gondwana is suggested by overall similarities between New Zealand intraplate volcanic rocks and volcanic rocks in East Australia and Antarctica. The petrogenetic model

Communicated by J. Hoefs.

Electronic supplementary material The online version of this article (doi:10.1007/s00410-006-0169-1) contains supplementary material, which is available to authorized users.

P. Sprung (✉)
Institut für Mineralogie,
Westfälische Wilhelms-Universität Münster,
Corrensstrasse 24, 48149 Münster, Germany
e-mail: sprungp@uni-muenster.de

S. Schuth · C. Münker
Mineralogisch-Petrologisches Institut,
Rheinische Friedrich-Wilhelms-Universität Bonn,
Poppelsdorfer Schloss, 53115 Bonn, Germany

L. Hoke
School of Earth Sciences, Victoria University of Wellington,
Kelburn Campus, Wellington, New Zealand

proposed here may therefore serve as a general model for the petrogenesis of Cretaceous to Recent intraplate volcanic rocks in former East Gondwana.

Introduction

Despite the widespread occurrence of continental intraplate volcanism, its origin and the nature of potential source regions are still contentious. A key question is whether the source regions are dominated by the hydrous subcontinental lithospheric mantle (SCLM) (e.g. Gallagher and Hawkesworth 1992; Hawkesworth and Gallagher 1993) or by the asthenospheric mantle with only minor contributions from the SCLM (e.g. McKenzie and Bickle 1988; White and McKenzie 1989). Lithospheric extension, shearing and transtensional decompression or heating by rising asthenospheric plumes are generally accepted mechanisms causing melting in intraplate regimes (e.g. Turcotte and Emerman 1983; White and McKenzie 1989; Vaughan and Scarrow 2003). For the generation of melts, metasomatised, heterogeneous lithospheric mantle with veins that are highly enriched in incompatible elements and have a low solidus temperature may play a significant role (Foley 1992; Mitchell 1995).

In the Cenozoic geological record of the New Zealand continental fragment (''Zealandia'', Luyéndyk 1995), both volcanism related to subduction and intraplate volcanism are common (Weaver and Smith 1989). A variety of models explain the origin of intraplate volcanism in Zealandia and the broader SW pacific area. For the South Island of New Zealand and the Chatham Islands, models involving active plumes (Adams 1981), plumelets (e.g. Weaver et al. 1994), metasomatised source regions (Gamble et al. 1986), or lithospheric sources (e.g. Weaver et al. 1994; Finn et al. 2005) with fossil plume signatures (Weaver et al. 1994) have been proposed. The intraplate provinces on the North Island have been related to ascending mantle plumes (Heming 1980a, b; Rafferty and Heming 1979), spatially distinct lithospheric sources (Cook et al. 2005), ascending mantle convection behind the active trench-arc complex (Heming and Barnet 1986) and spatially distinct source regions within the upper mantle (Huang et al. 2000).

As for Zealandia, a number of models have been used to explain the origin of geochemically diverse continental and oceanic intraplate volcanic fields that are common in the SW Pacific area. Both, lithospheric and asthenospheric sources, including plumes and layered mantle regimes have been proposed (e.g. Lanyon et al. 1993; Storey et al. 1999, Rocholl et al. 1995; Zhang et al. 2001; O'Reilly and Zhang 1995; Hart et al. 1995, 1997; Panter et al. 2000; Sprung et al. 2005). In an integrated geophysical and geochemical approach, similarities between these intraplate volcanic provinces have been attributed to the presence of old, metasomatised Gondwana SCLM in the source regions (Finn et al. 2005).

Here, we present a coherent major, trace element and Hf-Nd-Sr-Pb-isotope dataset obtained for mafic end members of intraplate volcanic fields throughout Zealandia. Our data are used to constrain the source regions of the volcanic fields, to assess potential regional variations, and to evaluate the control of the plate tectonic setting on the compositional diversity of the volcanic fields. A regional comparison corroborates the widespread occurrence of Gondwana SCLM in the source regions of volcanic fields throughout former East Gondwana.

Geological setting

Only about 10% of the New Zealand microcontinent (Fig. 1) are raised above sea level. The continental basement of New Zealand was formed during nearly continuous Cambrian to early Cretaceous convergence and subduction along the East Gondwana margin (e.g. Mortimer 2004). Since the breakup of East Gondwana in the Cretaceous that was linked to subduction of the Phoenix ridge and mantle plume activity (Storey et al. 1999; Weaver et al. 1994), Zealandia is separated from present day Australia. Rifting is inferred to have commenced by ~110 Ma (Waight et al. 1998), culminating in the formation of the Tasman Sea between ~85 (e.g. Li and Powell 2001) and ~60 Ma to ~53 Ma (Weissel and Hayes 1977; Kamp 1986). Zealandia's separation from present day Antarctica happened stepwise, ranging from ~120 to ~80 Ma along the Chatham Rise and ~83 to ~79 Ma in the Campbell Plateau area (e.g. Eagles et al. 2004).

At present, Zealandia is truncated by the obliquely convergent plate boundary between the Pacific Plate on the eastern side and the Indian-Australian Plate on the western side (Fig. 1). The new plate boundary evolved by ~45 Ma, when an oblique spreading zone propagated into Zealandia, possibly along a pre-existing Palaeozoic zone of lithospheric weakness (Sutherland 1999a; Sutherland et al. 2000). The spreading zone had evolved into a zone of oblique convergence by ~23 Ma (e.g. King 2000). Prior to ~6 Ma, when the major episode of compression forming the Southern Alps began, movement along the plate boundary was

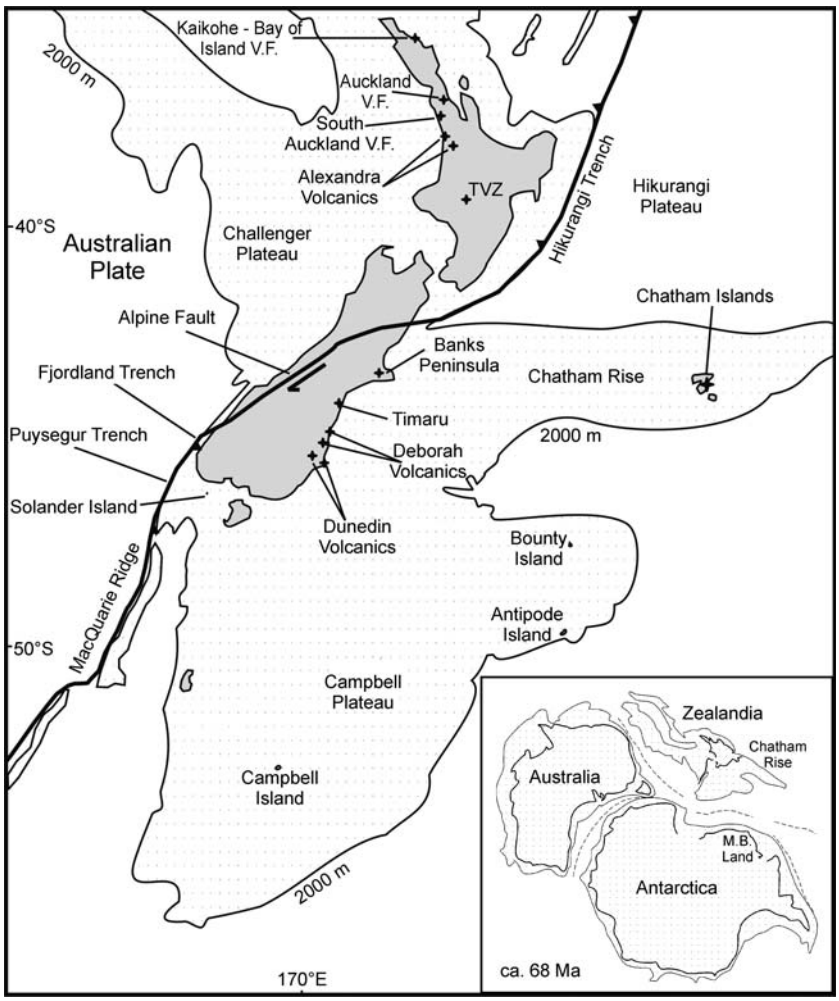

Fig. 1 Tectonic overview on the New Zealand microcontinent (Zealandia), its submarine extent, and the intraplate volcanic fields sampled (*black stars*). After Sutherland (1999a). *Inset*: Post breakup configuration (~68 Ma) of East Gondwana after Steinberger et al. (2004). *Dashed lines* illustrate active spreading ridges, dotted signatures delineate the approximate extent of the respective crustal segments

predominantly dextral strike-slip (e.g. Sutherland 1999b). Since ~12 Ma, the plate boundary links two inversely directed oblique subduction zones via the Alpine Fault, a zone of almost pure strike-slip motion truncating the South Island (e.g. King 2000; Sutherland 1999b).

A specific feature of the New Zealand microcontinent is the close temporal and spatial association of arc volcanism and intraplate volcanism. Ongoing westward subduction of the Pacific Plate along the Hikurangi subduction zone since ~30 Ma to the east of the North Island led to intermittent subduction related volcanism on the North Island since ~25 Ma (e.g. King 2000). For the area west of the recent arc chain, active back-arc spreading and rifting have been postulated (Hodder 1984; Spörli 1980; Stern 1985). On the South Island, no subduction related volcanism has been reported. Adakites on Solander Island south of the South Island (Reay and Parkinson 1997) are the northernmost extension of volcanism related to the eastward subduction of the Indian–Australian plate along the young (~12 Ma) Puysegur and Fjordland subduction zones (e.g. Lebrun et al. 2000; Sutherland 1995).

Intraplate volcanic and intrusive rocks occur throughout Zealandia (e.g. Weaver and Smith 1989, Hoke et al. 2000). On the South Island, intraplate volcanism was spatially diffuse, intermittent (mid-Cretaceous - Pliocene), and is characterised by relatively low volumes of erupted magma (e.g. Baker et al. 1994; Hoke et al. 2000; Weaver and Smith 1989). As volumetrically largest centres of volcanic activity, the Miocene Banks Peninsula (~11–5.8 Ma, ~1,800 km^3) near Christchurch and the Dunedin Volcano (~13–10 Ma, 80–150 km^3) at Dunedin stand out (e.g. Weaver and Smith 1989). In contrast, intraplate volcanism on the North Island is confined to two major extensional domains located behind the active volcanic arc (e.g. Hodder 1984; Spörli 1980; Weaver and Smith 1989). Within the Northland Volcanic Province, volcanic activity occurred between 9.7 Ma and 13 ka (Smith et al. 1993). The Auckland volcanic field (2.69 Ma–500 a) consist of a series of volcanic fields that decrease in age towards the north

(Briggs et al. 1989, 1994). The volcanic activity has been related to membrane stress (Hodder 1984) and propagating fractures in the lithospheric mantle (Cook 2002), similar to models proposed for oceanic intraplate volcanism that is not related to hotspots (e.g. Hieronymus and Bercovici 1999, 2000). The Chatham Islands on the eastern margin of Zealandia display three major episodes of mafic, highly undersaturated alkaline intraplate volcanism (Gamble et al. 1986; Grindley et al. 1977) between 85–82 Ma, 41–35 Ma, and ~5 Ma (Panter et al. 2006).

Sampling and analytical methods

Mafic samples of ten volcanic fields throughout New Zealand and the Chatham Islands have been sampled in order to obtain a temporally and spatially representative sample suite. Fresh samples were taken, avoiding alteration rims, veins, and xenoliths. Any remaining visible signs of alteration were removed. All samples were ground in an agate mill.

Based on thin section observation, a set of 23 fresh samples with negligible signs of alteration was chosen for analysis. Whole rock major element compositions and concentrations of V, Cr, Co, Ni, Rb, Sr, Zr and Nb were determined by X-ray fluorescence spectrometry (XRF) using a Philips PW-1480 at Universität Bonn. Fe^{2+}/Fe^{3+} was determined by titration (Heinrichs and Hermann 1990) at an external reproducibility of 5%. A subset of the 16 most primitive samples was additionally analysed for their trace element contents by quadrupole inductively coupled plasma mass spectrometry (ICP-MS) at Universität Kiel using an AGILENT 7500cs (see Schuth et al. 2004) with typical external reproducibility of 5–10% for most elements of interest. Differences between two separately digested duplicates of one sample (NZ 560A) were below 2% for all elements of interest. Measured concentrations for the BHVO-1 standard were generally within 10% of literature values for most elements of interest (Hf, Nb, Ta, Zr: Münker et al. 2003; Ba, Rb, Sr: Pin 2003; all other elements: Govindaraju 1994). For V, Cr, Co, Ni, Rb, Sr, Zr and Nb, most XRF- and ICP-MS-data agree to within <20% which is within the typical external reproducibilities of both methods. Major and trace element data are given in Table 1 of the electronic supplementary material.

Whole rock Hf–Nd–Sr–Pb isotope compositions were obtained for the 16 most primitive samples at Universität Münster. Hafnium, Nd, and Sr compositions were determined on the same split of ~ 150 mg rock powder. Lead isotope analyses were performed on small handpicked rock chips that were treated with ultrasound in deionised H_2O and leached for 1 h in hot 3 N HCl and 6 N HCl, respectively. For two samples with eruption ages of ~80 Ma, corrections for radiogenic ingrowths have been applied. The respective Pb isotope data were corrected using a typical μ of 8. For concentration measurements by isotope dilution (ID), mixed spike-solutions (^{87}Rb-^{84}Sr, ^{149}Sm-^{150}Nd, ^{176}Lu-^{180}Hf) were added to the two samples prior to digestion. Digestions followed a method described in Münker et al. (2001). An aliquot of the sample solution was taken for Hf and Lu separation using Eichron Ln-Spec resin (Münker et al. 2001). Rubidium, Sr, Sm and Nd were separated in a sequential column chemistry using cation-exchange resin (Dowex AG 50W × 8, 200–400 mesh) to extract Rb, Sr, and the REE fraction and a HDEHP based resin for Sm and Nd (Richard et al. 1976). For Pb separation, an HCl-HBr column chemistry using Dowex 1-X8 resin was applied (Manhes et al. 1984; Mattinson 1986; Tilton 1973). Lutetium and Hf isotope analyses were run on a Micromass Isoprobe (MC-ICPMS). Neodymium, Sm, Sr were analysed on a Finnigan Triton (MC-TIMS), Rb on the Micromass VG Sector 54 (MC-TIMS). Lead isotope compositions were determined both with a Finnigan Triton and a Micromass VG Sector 54. All analyses were run in static mode. An external correction for mass bias using repeated runs of NBS 982 that were normalised to accepted values (Todt et al. 1996) was applied to all Pb isotope data (~0.1% per amu). The external reproducibility deduced from our NBS 982 runs was ~0.05% per amu (2 RSD). Hafnium, Nd and Sr isotope values were internally corrected for mass fractionation using the exponential law and the following normalising values: $^{86}Sr/^{88}Sr = 0.1194$, $^{146}Nd/^{144}Nd = 0.7219$, and $^{179}Hf/^{177}Hf = 0.7325$. For fractionation correction of Lu, $^{176}Lu/^{175}Lu$ was normalised to the measured $^{187}Re/^{185}Re$ of doped Re (Scherer et al. 1999). No analytically significant fractionation correction was required for Rb measurements (external reproducibility ±1%). All $^{176}Hf/^{177}Hf$ values are given relative to a $^{176}Hf/^{177}Hf$ value of 0.282160 for the JMC-475 standard at a long-term external reproducibility of ±50 ppm. For Nd isotope analyses, a long-term external reproducibility of ±30 ppm is achieved with the Finnigan Triton at Münster. Repeated measurements of the La Jolla standard ($n = 5$) gave a $^{143}Nd/^{144}Nd$ of 0.511839 ± 0.000014 (2σ). The long-term external reproducibility for $^{87}Sr/^{86}Sr$ with the Finnigan Triton at Münster is ±40 ppm. Repeated runs of NBS 987 ($n = 7$) yielded a $^{87}Sr/^{86}Sr$ of 0.710253 ± 0.000032 (2σ). The external

precision for Lu/Hf and Rb/Sr is ±1 and ±0.2% for Sm/Nd. Average deviations of the concentrations determined by ICPMS from isotope dilution data are generally below 5% except for Sr concentrations (~9.5%). Blanks determined in the course of analyses were 12 pg for Hf, 115 pg for Nd, 165 pg for Sm, and ca. 400 pg for Pb. Strontium blanks are typically ~50 pg. All procedural blanks are negligible with respect to the sample concentrations.

The chondritic parameters and decay constants used for calculations of εNd and εHf values and age corrections are: $^{143}Nd/^{144}Nd = 0.512638$, $^{147}Sm/^{144}Nd = 0.1967$ (Jacobsen and Wasserburg 1980; Wasserburg et al. 1981)), $\lambda^{147}Sm = 6.54 \times 10^{-12}$ (Lugmair and Marti 1978), $^{176}Hf/^{177}Hf = 0.282772$, $^{176}Lu/^{177}Hf = 0.0332$ (Blichert-Toft and Albarède 1997), $\lambda^{176}Lu = 1.865 \times 10^{-11}$ a^{-1} (Scherer et al. 2001), $\lambda^{87}Rb = 1.42 \times 10^{-11}$ a^{-1}, $\lambda^{238}U = 1.55125 \times 10^{-10}$ a^{-1}, $\lambda^{235}U = 9.8485 \times 10^{-10}$ a^{-1}, and $\lambda^{232}Th = 4.9475 \times 10^{-11}$ a^{-1} (Steiger and Jäger 1977). All isotope data are given in Table 1, concentration determinations and age corrected data are given in Table 2 of the electronic supplementary material.

Results

Petrography

All samples are volcanic or shallow intrusive rocks. In thin section, most samples display a microcrystalline to vitric matrix with phenocrysts of clinopyroxene, plagioclase and subordinate magnetite or ilmenite. Minor iddingsite rims on olivine crystals have been observed in some cases. Two samples (NZ 553, NZ 557) contained peridotitic mantle xenoliths, which were carefully removed. Xenocrystic olivine showing kink bands is present in three samples (NZ 58 CH, NZ 570 A, D 113). One sample shows abundant idiomorphic clinopyroxene (NZ 560 A). Hornblende is only present as partially resorbed, metastable xenocrysts in one sample from the Chatham Islands (NZ 39 CH B).

Geochemistry

Major and trace elements: whole data set

Following the IUGS classification scheme for igneous rocks (Le Maître et al. 1989) sample compositions vary between basanitic, andesitic and mugearitic (not shown). Basanites and basalts are the dominant rock types. Major element contents used in plots and reported in the text are recalculated on a volatile-free basis. MgO-contents vary from ~4.0 to 13.5 wt.-%, Mg# from ~52 to 75. The overall range for Ni- and Cr-contents is 37–364 ppm and 30–605 ppm, respectively, both showing positive correlations with MgO and Mg# for the whole data set as do V and Co (not shown). Total iron contents (Fe_2O_3t) vary between 8.1 and 13.8 wt.-%, CaO/Al_2O_3 ranges from 0.51-0.88. Both, Fe_2O_3t and CaO/Al_2O_3 display negative trends with SiO_2 (Fig. 2) and a broad positive trend with MgO (not shown). Generally, incompatible major and trace element contents display negative correlations with SiO_2 (Fig. 2).

Table 1 Hf–Nd–Pb–Sr isotope data obtained by TIMS and MC-ICPMS analyses

Sample	$^{176}Hf/^{177}Hf$	ε Hf	$^{87}Sr/^{86}Sr$	$^{143}Nd/^{144}Nd$	ε Nd	$^{206}Pb/^{204}Pb$	$^{207}Pb/^{204}Pb$	$^{208}Pb/^{204}Pb$
NZ39 CHB	0.282997 ± 6	+7.9	0.703465 ± 13	0.512885 ± 15	+4.8	20.51	15.75	40.43
NZ58 CH	0.282830 ± 5	+3.8	0.702969 ± 15	0.512750 ± 11	+4.2	20.57	15.77	40.14
NZ64 CH	0.282834 ± 5	+4.0	0.703038 ± 14	0.512775 ± 9	+4.6	19.93	15.75	39.73
NZ552	0.282895 ± 7	+4.4	0.703704 ± 16	0.512838 ± 12	+3.9	18.99	15.67	38.96
NZ555	0.282896 ± 8	+4.4	0.703400 ± 15	0.512863 ± 12	+4.4	19.18	15.69	38.97
NZ553	0.282988 ± 5	+7.6	0.702887 ± 14	0.512921 ± 10	+5.5	19.90	15.68	39.48
NZ557	0.282980 ± 7	+7.4	0.702841 ± 14	0.512890 ± 10	+4.9	20.28	15.69	39.81
NZ560 A	0.282944 ± 6	+6.1	0.703330 ± 13	0.512849 ± 10	+4.1	19.52	15.66	39.24
D113	0.282988 ± 6	+7.7	0.703611 ± 14	0.512884 ± 12	+4.8	19.16	15.65	39.02
D117	0.283036 ± 7	+9.3	0.703096 ± 13	0.512942 ± 10	+5.9	19.63	15.65	39.46
NZ568	0.282987 ± 6	+7.6	0.703154 ± 15	0.512915 ± 12	+5.4	19.11	15.60	38.80
NZ569	0.282988 ± 7	+7.6	0.702782 ± 13	0.512973 ± 10	+6.5	19.37	15.60	38.98
NZ570 A	0.282987 ± 6	+7.6	0.702889 ± 14	0.512970 ± 11	+6.5	19.31	15.62	39.02
NZ566	0.283052 ± 6	+9.9	0.702811 ± 16	0.512996 ± 15	+7.0	19.01	15.62	38.73
NZ573	0.283003 ± 6	+8.2	0.702836 ± 16	0.512972 ± 9	+6.5	19.28	15.61	38.90
NZ575	0.283006 ± 9	+8.3	0.702758 ± 14	0.512971 ± 9	+6.5	19.34	15.60	38.95

Isotope data for NZ 58 CH and NZ 64 CH are corrected for radiogenic ingrowths as presented in Table 2 of the electronic supplementary material, Pb isotope data for both samples are recalculated assuming a μ-value of 8

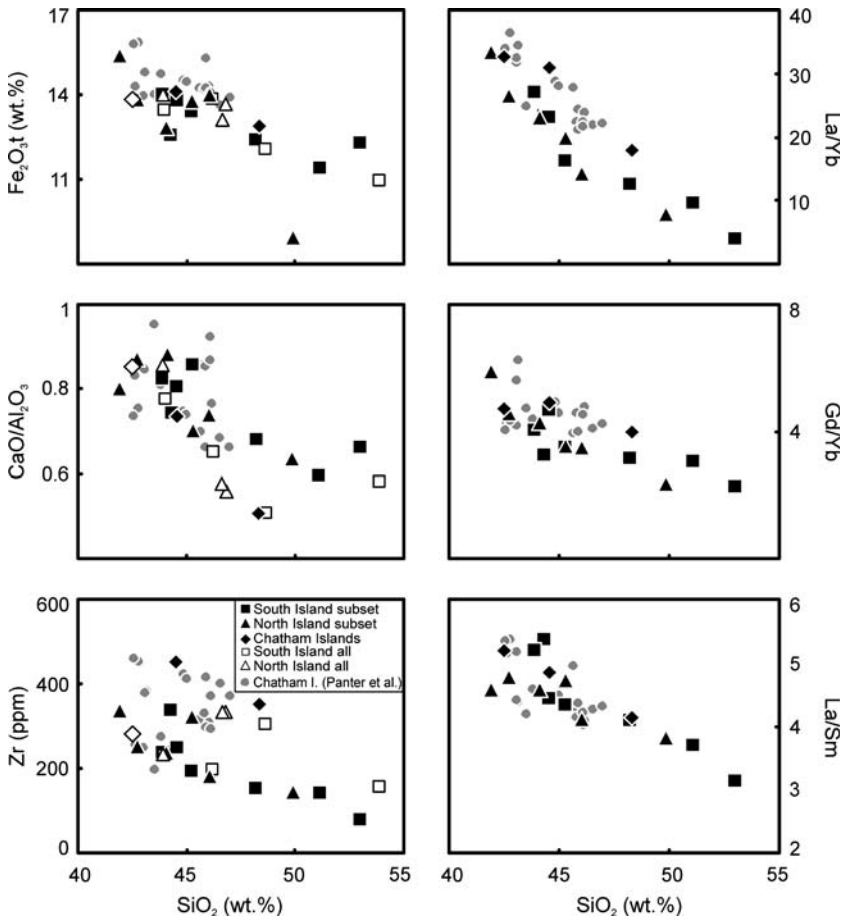

Fig. 2 Major and trace element variations with SiO_2. *Solid symbols*: subset of most primitive samples analysed by ICP-MS; *open symbols*: other samples analysed by XRF. *Triangles*: North Island; *squares*: South Island; *diamonds*: Chatham Islands. *Light grey filled circles* are data for the Chatham Islands from Panter et al. (2006). Gd concentrations of the Panter et al. data are extrapolated from the geometrical mean of neighbouring elements on a PM normalised multi element diagram

Major and trace elements: subset of most primitive samples

Based on major element compositions, a representative subset of the 16 most primitive samples (Mg# > 62, MgO > 7 wt.-%, Ni > 80 ppm, and Cr > 230 ppm) from the different intraplate volcanic fields was chosen to characterise source compositions. Despite its low MgO-, Ni, and Cr- contents (~ 4 wt.-%, 43 and 34 ppm respectively), sample NZ 64 CH was included in order to extend the isotope data set for the Chatham Islands. Furthermore, despite showing some effects of fractionation and crustal assimilation, the data of Panter et al. (2006) for the Chatham Islands have been included. Within this subset, negative correlations of Fe_2O_3t, CaO/Al_2O_3 and incompatible element concentrations with SiO_2 are even more pronounced both on a regional and a Zealandia wide scale (filled symbols in Fig. 2). Incompatible trace element and LREE concentrations display large variations (La_N/Yb_N = 2.7–22.4; normalised to chondritic values of Boynton (1984)) and show clear negative correlations with silica contents as do La/Yb, La/Sm, and Gd/Yb (Fig. 2). Our samples from the Chatham Islands and some samples from the South Island are most enriched in incompatible elements (Fig. 3). There are considerable variations in the degree of trace element enrichment within the South Island subset. Even the most enriched samples from the North Island display lower concentrations of incompatible elements than enriched samples from the South Island and the Chatham Islands. Primitive mantle normalised multi element diagrams of the highly enriched samples strongly resemble those of HIMU-OIB (Fig. 3). Generally, there are maxima for Nb-Ta and Th-U. Within the South Island subset, Nb-Ta gets increasingly depleted relative to U-Th with decreasing degree of trace element enrichment, resulting in a positive trend of Nb/Th with La/Yb. All samples show distinct negative anomalies for K and Pb relative to elements of similar incompatibility. K/Ce, K/K* and Pb/Pb* are negatively correlated with La/Yb (Fig. 4). To a lesser extent, Hf displays negative anomalies, resulting in highly fractionated values of Zr/Hf (35–55). For the South Island data set, Zr/Hf show a positive trend with La/Yb (Fig. 4).

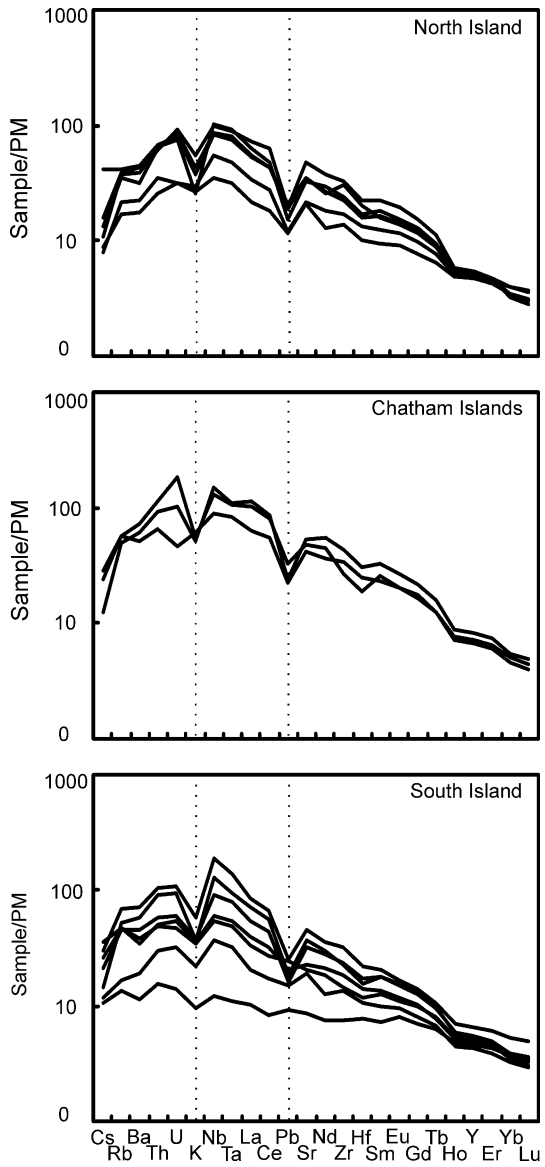

Fig. 3 Primitive Mantle (McDonough and Sun 1995) normalised multi element variation diagrams. From top to bottom: North Island: NZ 569, NZ 575, NZ 570A, NZ 568, NZ 573, NZ 566; Chatham Islands: NZ 39 CH B, NZ 58 CH, NZ 64 CH; South Island: NZ 553, NZ 557, D 117, NZ 560 A, D113, NZ 555, NZ 552

Hf–Nd–Pb–Sr Isotope compositions

Within our dataset, there are distinct regional variations in the isotope composition of Hf, Nd, Sr, and Pb (Figs. 5, 6). The North Island subset is relatively homogeneous. North Island data plot close to or within the enriched ends of the depleted mantle field in εHf vs. εNd, $^{207}Pb/^{204}Pb$ vs. $^{206}Pb/^{204}Pb$ and $^{87}Sr/^{86}Sr$ vs. $^{206}Pb/^{204}Pb$ diagrams. Chatham Island data (including the data of Panter et al. (2006)) cluster around the field of the HIMU mantle end member (Zindler and Hart 1986). The radiogenic $^{206}Pb/^{204}Pb$-signature (up to 20.5) is persistent over the whole time span of volcanic activity on the Chatham Islands (~80 Myrs) (Fig. 7). Within the South Island subset, isotope compositions are less homogeneous. In $^{87}Sr/^{86}Sr$ versus $^{206}Pb/^{204}Pb$ space, the data fall on a trend ranging from HIMU into the field of the depleted mantle, but also show an influence of a component with distinctly radiogenic $^{87}Sr/^{86}Sr$. A similar trend is observed in $^{207}Pb/^{204}Pb$ versus $^{206}Pb/^{204}Pb$ space, where two samples yield $^{207}Pb/^{204}Pb$ values even beyond the field for the EM-2 mantle end member (Zindler and Hart 1986), pointing towards the direction of GLOSS (Global Subducting Sediments, Plank and Langmuir 1998). Notably, these two samples are the youngest and the oldest sample of the South Island subset (Fig. 7). A trend to less radiogenic $^{206}Pb/^{204}Pb$ with decreasing age exists for the South Island samples that are younger than ~20 Ma. In εHf versus εNd space, all samples fall within the range of HIMU (e.g. Stracke et al. 2003). Only the South Island subset displays clear correlations of isotope compositions with silica contents and La/Yb (Fig. 4). The samples that are the lowest in silica content and the most enriched in incompatible elements are isotopically closest to HIMU. Notably, Zr/Hf also display a distinct positive trend with $^{206}Pb/^{204}Pb$ (not shown). No systematic variations of isotope compositions with MgO-contents (Fig. 1 electronic supplementary material) or Mg# (not shown) have been observed for our data set. Samples from the Chatham Islands constitute a suitable end member to the trends defined by the South Island subset.

Discussion

Fractional crystallisation and crustal assimilation

Constraining the mantle source characteristics of volcanic rocks relies on the near primary nature of the analysed samples, for which low silica contents (<55 wt.-%), MgO contents above 6 wt.-%, Mg# above 68 and Ni and Cr contents significantly above 100 ppm are frequently used as criteria. Yet, considerable variations in Ni and Cr contents can be produced by melting of a metasomatically enriched mantle peridotite or by melting of a drastically depleted mantle peridotite (e.g. McKenzie 1989; Halliday et al. 1995; Hirschmann et al. 2003; Kogiso et al. 2003, 2004, Bogaard and Wörner 2003). In particular, melting of pyroxenite veins can generate primary basanitic to dacitic melts with Mg# varying from 75 to 60 and less (Kogiso et al. 2004). Hence, variable silica contents and Mg# as observed for

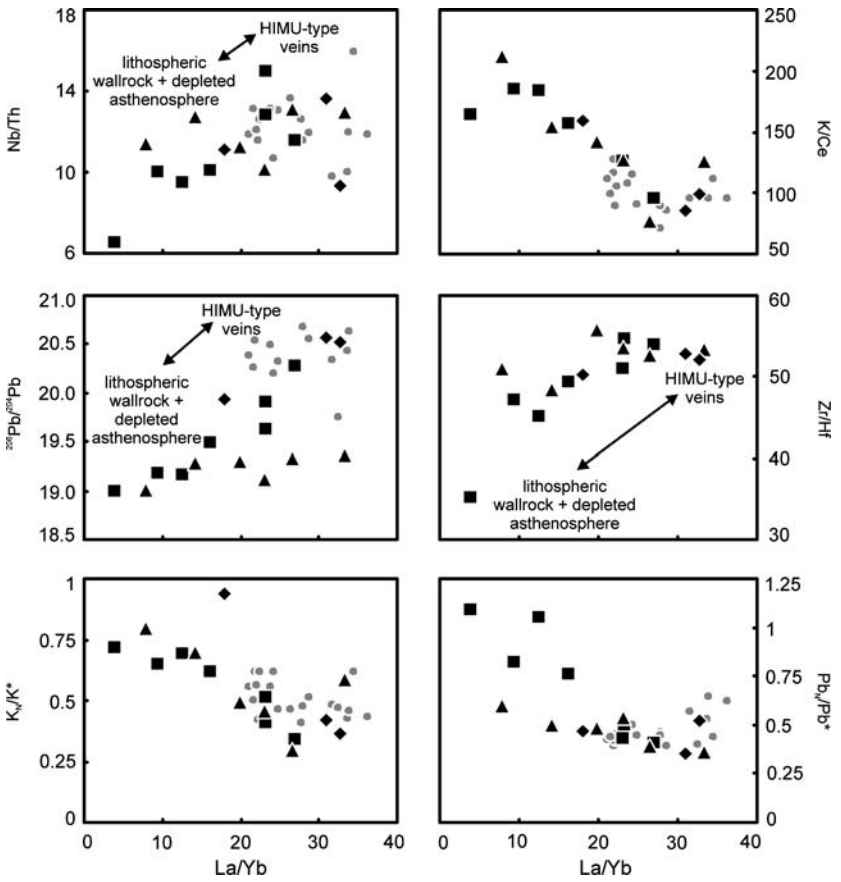

Fig. 4 Plots of Nb/Th, $^{206}Pb/^{204}Pb$, K/Ce, Zr/Hf, K/K*, and Pb/Pb* versus La/Yb. K* and Pb* are the extrapolated concentrations calculated from the geometrical mean of neighbouring elements on a PM normalised multi element diagram. *Symbols* are the same as in Fig. 2

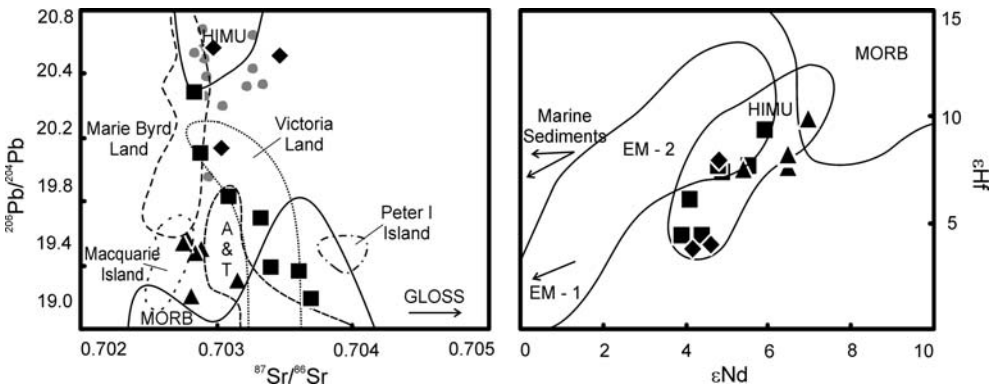

Fig. 5 Plot of $^{206}Pb/^{204}Pb$ vs. $^{87}Sr/^{86}Sr$ and εHf vs. εNd. Fields for volcanic provinces in the SW Pacific and Eastern Australia are from the compilation of Finn et al. (2005); mantle end members and MORB from an updated compilation of Stracke et al. (2003, 2005) approximate εHf and εNd compositions of ''Marine Sediments'' (Vervoort et al. 1999) and EM-1 (after Stracke et al. 2003) are indicated by arrows. A & T is ''Australia and Tasmania''; GLOSS is ''Global subducting sediment'' (Plank and Langmuir 1998). *Symbols* are the same as in Fig. 2

our dataset not necessarily need to be the result of crystal fractionation or crustal assimilation. A lack of negative Eu-anomalies, decreasing Ni, Cr, and V contents with decreasing Mg# and MgO contents, and increasing Al_2O_3 contents with decreasing MgO contents (not shown) are in principle in agreement with fractionation of olivine and clinopyroxene. In contrast to this, the observed negative correlations of incompatible trace elements with silica contents are inconsistent with typical fractional crystallisation trends (Fig. 2), as confirmed by the subset of primitive samples, where these trends are even more pronounced.

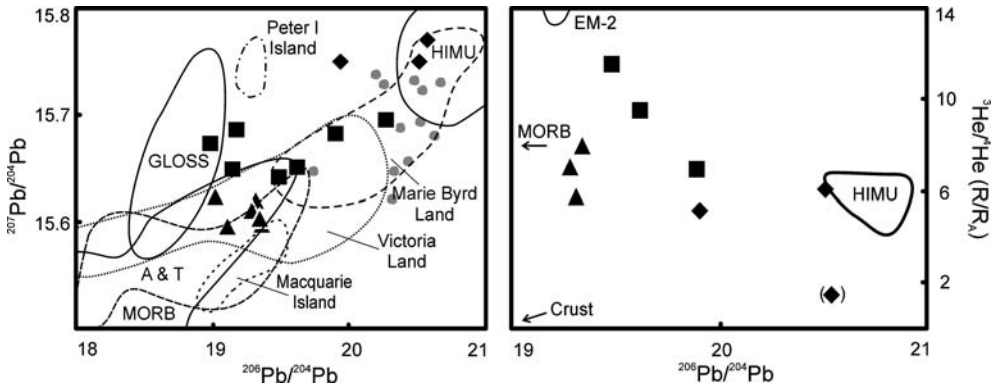

Fig. 6 Plot of $^{207}Pb/^{204}Pb$ versus $^{206}Pb/^{204}Pb$ and $^{3}He/^{4}He$ (R/R_A) versus $^{206}Pb/^{204}Pb$. Fields for volcanic provinces in the SW Pacific and Eastern Australia are from the compilation of Finn et al. (2005); mantle end members and MORB from an updated compilation of Stracke et al. (2003); typical Helium isotope data (R/Ra) for HIMU (St.Helena), EM-2 (Tonga) and MORB are from Graham (2002); He data for our analysed samples from the South Island and the Chatham Islands are from Hoke et al. (2000), data for North Island locations are from Patterson et al. (1994); *symbol in brackets*: He data from xenoliths. A & T is ''Australia and Tasmania''. *Symbols* are the same as in Fig. 2

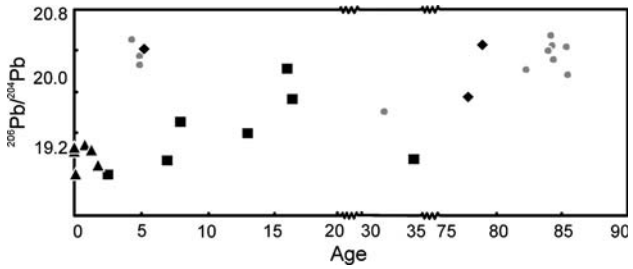

Fig. 7 $^{206}Pb/^{204}Pb$ versus approximate eruption age (in Ma) for all samples analysed. Detailed age informations and references are given in Table 1 of the electronic supplementary material. *Symbols* are the same as in Fig. 2

Several lines of evidence argue against crustal contamination as a controlling factor of the elemental and isotopic composition of our subset of samples. If the elevated silica contents were the consequence of crustal assimilation, this mechanism would also have to account for the concomitant decrease in incompatible trace element concentrations (Fig. 2). Given the incompatible trace element enriched composition of the continental crust (e.g. Rudnick and Gao 2003; Taylor and McLennan 1985), such a scenario is impossible, even for highly enriched intraplate magmas. Moreover, crustal contamination would have produced correlations of radiogenic isotope compositions with MgO contents, which is not observed for our data set (Fig. 1 electronic supplementary material).

In summary, neither crystal fractionation nor crustal contamination are mechanisms capable of producing the isotopic and trace element composition of our primitive subset of volcanic rocks. Although both processes cannot entirely be ruled out, significant effects on the sample compositions can be excluded.

Melting depths and melting degrees

The observed negative correlations of incompatible elements and Fe_2O_3t with SiO_2 (Fig. 2) can be attributed to varying degrees of melting, caused by variable melting depths. Generally, low degree melts are generated at greater depths and show lower silica contents, higher total iron contents and a stronger enrichment in incompatible trace elements than higher degree melts (e.g. Langmuir et al. 1992). Additionally, as observed for our data set, CaO/Al_2O_3 that are negatively correlated with SiO_2 (Fig. 2) indicate increasing melting depths in the presence of garnet (Herzberg 1995; Walter 1998). Since the source regions of intraplate volcanism have been suggested to contain both, volatiles and mafic lithologies (e.g. Dasgupta et al. 2006; Gallagher and Hawkesworth 1992), it is of importance to note, that for primary melts of hydrous peridotite and carbonated eclogite (Asimow and Langmuir 2003; Asimow et al. 2004; Dasgupta et al. 2006) comparable compositional trends result from changing melting depths.

The relationship between melting depth and degree of melting can further be tested using the LREE enrichment as an indicator for varying degrees of melting and HREE depletion as an indicator for the impact of residual garnet (e.g. van Westrenen et al. 2001a, b). As the effect of garnet on REE partitioning is relatively insensitive to the presence of H_2O (Wood and Blundy 2002), the observed negative correlations of La/Sm, La/Yb, and Gd/Yb with SiO_2 (Fig. 2) strongly argue for varying melting depths in the presence of garnet as the controlling factor for the degree of melting independent from the potential source characteristics.

Further constraints on the melting depth and the influence of residual garnet can be made from the different behaviour of Sm/Nd and Lu/Hf during mantle melting (Fig. 8). Due to the high compatibility of Lu in mantle garnet (e.g. van Westrenen et al. 2001a, b), partial melting in the garnet stability field fractionates Lu/Hf stronger than Sm/Nd. In contrast, Sm/Nd and Lu/Hf in the spinel stability field are largely controlled by clinopyroxene, resulting in a strong coupling of both ratios (cf. Chauvel and Blichert-Toft 2001). Minor volatile rich phases in the lithospheric mantle such as phlogopite or amphibole either (phlogopite) do not have sufficiently high partition coefficients to affect both element ratios significantly or (amphibole) do not differ significantly from clinopyroxene in their respective fractionation behaviour (e.g. LaTourrette et al. 1995; Ionov et al. 1997; Hart and Dunn 1993). Calculated melting curves for Lu/Hf and Sm/Nd, assuming accumulated fractional melting (Shaw 1970), for the spinel and the garnet stability field bracket all of our data for intraplate samples from New Zealand. Hence, pooling of polybaric melts originating from both the spinel and garnet stability fields is a viable mechanism (cf. Chauvel and Blichert-Toft 2001). Consequently, the variation in melting depths inferred for our data set can be interpreted in terms of a melting column model, reflecting variable average melting depths (Langmuir et al. 1992).

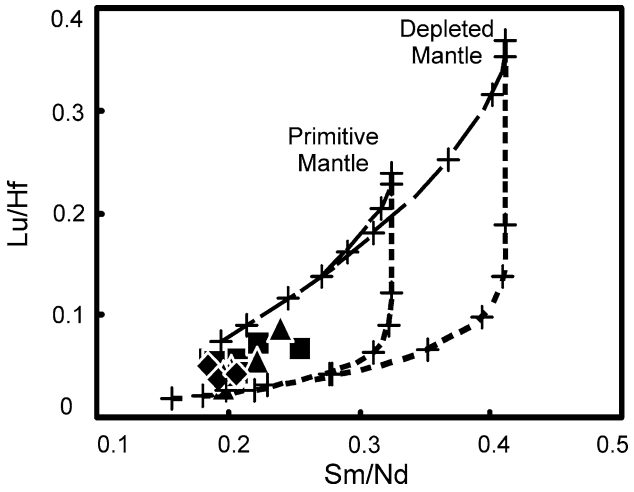

Fig. 8 Plot of measured Lu/Hf versus Sm/Nd with modelled melting curves for accumulated fractional melting within the spinel (*long dashed lines*) and the garnet stability field (*short dashed lines*). Starting compositions are trace element contents for the primitive mantle (McDonough and Sun 1995) and the depleted mantle (Workman and Hart 2005). Source mineralogy, melting modes and selection of partition coefficients are from Chauvel and Blichert-Toft (2001). Melting steps are at 0.1, 2, 5, 1, 15, 20 and 25%. *Symbols* are the same as in Fig. 2. Using other proposed depleted mantle values (e.g. Salters and Stracke (2004)) does not change the result significantly

Lithospheric versus asthenospheric sources

Two lines of evidence, both relying on distinct compositional differences between the asthenospheric and the lithospheric mantle, indicate that the New Zealand intraplate magmas are in part derived from the lithospheric mantle. These are (1) the presence of residual hydrous phases and (2) the long term persistence of distinct isotopically ''enriched'' source components. While volatile-rich mineral phases such as amphibole or phlogopite are stable at conditions of the lithospheric mantle (Wallace and Green 1991; Foley 1992; Class and Goldstein 1997) and have been described in xenoliths (e.g. Ionov et al. 1997), they are not stable in the convecting asthenosphere or in thermally anomalous plumes (Wallace and Green 1991; Class and Goldstein 1997). The observed negative anomalies of K and negative correlations of K/K* and K/Ce with La/Yb (Fig. 4) are in perfect agreement with the presence of a buffering residual K-rich (lithospheric) mineral phase during partial melting (Class and Goldstein 1997; Le Roex et al. 2001; Späth et al. 2001). Such buffering K-rich phases cause (1) K to behave less incompatibly during partial melting than elements of similar incompatibility and (2) nearly constant K contents at different degrees of partial melting (Späth et al. 2001). A decrease in K contents of partial melts buffered by K-rich phases will not happen until the complete consumption of the phase (Späth et al. 2001), which is hard to achieve due to solid solution melting in the presence of F (Foley 1991, 1992). As implied by the co-variation of K/K* and Pb/Pb*, K-Richterite may be the predominant volatile-rich mineral in the sources of the New Zealand magmas (Grégoire et al. 2002).

The SCLM does not take part in mantle convection and thus can act as a rigid and chemically isolated entity over geological time (e.g. Hawkesworth and Gallagher 1993; Wilson et al. 1995). Accordingly, as shown by isotope and trace element compositions of xenoliths from the SCLM (e.g. Handler et al. 2003, 2005; Ionov et al. 2006; McBride et al. 1996; O'Reilly and Zhang 1995; Zhang et al. 2001), the SCLM can preserve distinct geochemical heterogeneities such as those induced by subduction or by infiltration by asthenospheric melts (e.g. Hawkesworth et al. 1990; McKenzie 1989; Foley 1992). Despite the significant lateral transport of Zealandia since the Late Cretaceous (e.g. Weissel et al. 1977; Kamp 1986; Eagles et al. 2004; Panter et al. 2006), our new data together with previous studies (e.g. Baker et al. 1994; Panter et al. 2005, 2006; Sprung et al. 2005) demonstrate the regional persistence of ''HIMU-like'' isotope and trace element signatures throughout ~100 Ma of intermittent

volcanic activity (Fig. 7). Thus, these ''HIMU-like'' source components, identified by highly radiogenic $^{206}Pb/^{204}Pb$, have to reside within the lithospheric mantle. Likewise, isotope signatures that tend towards those of subducted sediments (high $^{87}Sr/^{86}Sr$ and high $^{207}Pb/^{204}Pb$) can be observed over the whole time span of volcanic activity on the South Island covered by our data set (Fig. 7). Similar to models for the East Australian SCLM (e.g. Zhang et al. 2001), the observed sediment-like signatures are best explained by a metasomatic enrichment of the SCLM with subduction components originating from the Paleozoic to Mesozoic history of subduction beneath East Gondwana. An increasing contribution from fossil subduction components is also confirmed by the decrease of Nb/Th (low in subduction components) with decreasing La/Yb displayed by the South Island samples (Fig. 4). Furthermore, the two samples with Pb and Sr compositions closest to those of pelagic sediments, in agreement with the smaller mobility of Nd and especially Hf in subduction components (e.g. Kogiso et al. 1997), display no shift from the HIMU field in εHf versus εNd space.

Altogether, these systematics imply a lithospheric origin of the enriched signatures in the New Zeland magmas (cf. Cook et al. 2005) and argue against an asthenospheric origin. Furthermore, EM-2 type mantle that also bears pelagic sediment-like signatures is less radiogenic in $^{207}Pb/^{204}Pb$ (e.g. Hofmann 1997) and is expected to display significantly higher $^{3}He/^{4}He$ (e.g. Graham 2002) than the Zealandia rocks. Although an increase in $^{3}He/^{4}He$ with decreasing $^{206}Pb/^{204}Pb$ is observed for the South Island subset (Fig. 6; Hoke et al. 2000), the temporal variation of He-isotope compositions does not support a plume involvement (Hoke et al. 2000).

The third isotopic end member that is particularly present in the North Island samples and that shows increasing influence with increasing degree of melting for the South Island data resembles the depleted mantle composition. Although the K contents in all magmas are buffered by hydrous phases of the lithospheric mantle, there is a general decrease in K with increasing degree of melting Zealandia wide (not shown). This feature can be explained by a mixed asthenospheric and lithospheric source region (cf. Ellam and Cox 1989; 1991; Gallagher and Hawkesworth 1992; Hawkesworth and Gallagher 1993), where the K-poor asthenospheric melts dilute the lithospheric components. According to the veined lithosphere model of Foley (1992), the trace element signatures of highly enriched lithospheric veins will still dominate the trace element inventory of melts, even if the degrees of melting and, accordingly, the asthenospheric contribution are high.

Relationship between melting depth and magma compositions

Whereas the base of the SCLM is in thermal equilibrium with the underlying asthenosphere (e.g. McKenzie et al. 2005), the temperature decreases rapidly with decreasing depth (e.g. Hawkesworth and Gallagher 1993). Hence, melting is restricted to the base of the SCLM where the geothermal gradient intersects the solidus (Wilson et al. 1995). Consequently, the average depth of a melt column that reaches into the SCLM provides an approximation of the lithospheric thickness. For the South Island subset, a distinct relationship between melting depth and isotope compositions can be documented by our data set. Negative correlations of $^{207}Pb/^{206}Pb$, $^{208}Pb/^{206}Pb$, and $^{87}Sr/^{86}Sr$ with La/Yb (not shown) as well as a strong positive correlation of $^{206}Pb/^{204}Pb$ with La/Yb (Fig. 4) indicate that the strongest affinities to HIMU are displayed by those samples that are derived from the greatest average melting depths. With decreasing melting depth, ''HIMU-like'' signatures are less pronounced and get replaced by depleted-mantle-like and sediment-like signatures. Sediment-like signatures are strongest in those samples that are derived from the shallowest average melting depth. As the lithospheric mantle is partly enriched in volatiles (e.g. Wilson et al. 1995), its solidus temperature is generally lower than that of dry asthenospheric peridotite (Green 1973; Olafsson and Eggler 1983, Falloon and Green 1990). Veins of frozen low degree asthenospheric melts highly enriched in incompatible elements (e.g. McKenzie 1989) are prone to melt prior to the surrounding lithospheric wall-rock (Foley 1992). Thus, the presence of frozen melt veins of ''HIMU-like'' compositions in the base of the lithospheric mantle that is modified by subduction components with sediment-like signatures, can explain the range of compositions found in the New Zealand magmas. The almost undiluted ''HIMU-like'' compositions of the Chatham Islands and South Island samples originate from low melting degrees at great average melting depths (i.e. largest lithospheric thickness). Melts with more pronounced sediment-like or asthenospheric signatures originate from shallower melting depths in regions where the lithosphere is less thick.

Despite clear variations in melting depth and the degree of melting, all compositions of the North Island samples resemble compositions of the depleted mantle and do not display major isotopic variations with

varying melting depths. This pattern implies a relatively constant proportion of melts derived from asthenospheric and lithospheric sources and a general predominance of depleted mantle sources. As further discussed below, this observation can be related to the tectonic setting of the North Island with elevated asthenospheric heat flow and high degrees of extension.

The evidence for a three component model is summarised by Nb/Th versus La/Sm systematics (Fig. 9). The model assumes mixing of typical melts derived from the three proposed source end members. The trend displayed by our South Island subset in Nb/Th versus La/Sm space cannot be explained by binary mixing between two of the pure end members, whereas mixing of the three components with varying proportions is a suitable process. Our interpretations inferred from Nb/Th versus La/Sm systematics are confirmed by modelling of trace element patterns (Fig. 9) where three source components can explain the observed patterns.

Petrogenetic model

Isotope and trace element variations in the New Zealand intraplate samples require an interplay of at least three components involving lithospheric and asthenospheric sources. The three components are: (1) Trace element enriched ''HIMU-like'' veins frozen in (2) a lithospheric mantle modified by old subduction components and (3) the depleted upper asthenospheric mantle. Following previous models (e.g. Gallagher and Hawkesworth 1992; Hawkesworth and Gallagher 1993), melting in the SCLM dominates at a large lithospheric thickness and very low extension rates. With decreasing lithospheric thickness, elevated rates of extension and a lower asthenospheric potential temperature, asthenospheric sources tend to dominate. For melting of a veined lithospheric mantle, the ''Vein-Plus-Wall-Rock'' melting model (Foley 1992) predicts an increasing impact of the lithospheric wall-rock and increasing asthenospheric contributions at high degrees of melting. These models can be applied to our melt column approach for the New Zealand intraplate rocks, thus requiring regionally different lithospheric thicknesses and different stress regimes in Zealandia. In combining magma compositions and tectonic setting, the Chatham Island samples, originating from a non-extensional regime far off the present plate boundary, show the strongest affinities to HIMU. These small degree melts are derived from great depth and predominantly tap the lithospheric vein assemblage, implying a large lithospheric thickness (Fig. 10). Signatures that resemble those of the depleted asthenosphere combined with more dilute ''HIMU-like'' trace element signatures are observed for the North Island subset. Including previously published data (Cook 2002; Cook et al. 2005; Huang et al. 1997, 2000), a minor contribution from subduction modified lithospheric wall-rock can also be observed. The lithospheric and asthenospheric source proportions appear to be relatively constant for the North Island, reflecting a tectonic regime with elevated heat flow behind the active trench-arc complex and an exten-

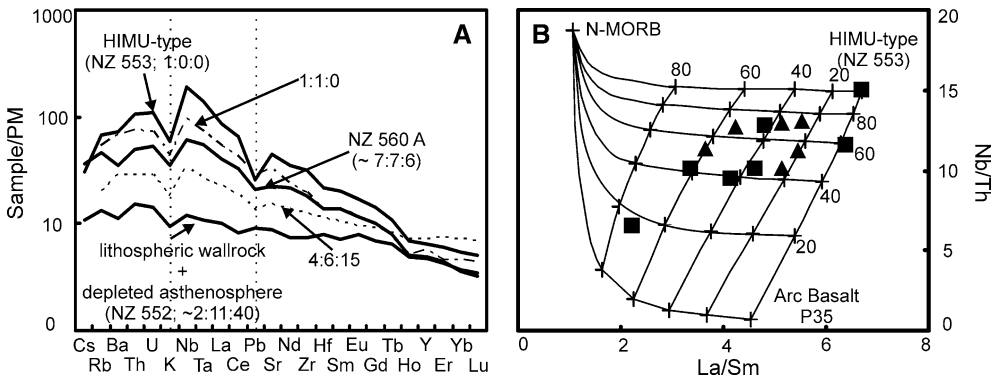

Fig. 9 Primitive mantle normalised multi element diagrams (**a**) and plots of Nb/Th versus La/Sm for the South Island and the North Island subsets (**b**), both illustrating three component mixing between typical N-MORB (Hofmann 1988), HIMU-type end member (sample NZ 553), and a primitive subduction related arc basalt (P35 of Briggs and McDonough 1990). Nb/Th versus La/Sm mixing lines in (**b**) have been calculated at constant contributions from N-MORB (0, 2%, 40%,...). NZ 552 and NZ 553 in (**a**) bracket the overall range of the South Island subset on multi element variation diagrams. Calculated trace element patterns represent proportions (HIMU end member: Subduction related basalt : N-MORB) of 1:1:0 (*dashed and dotted line*) and 4:6:15 (*dotted line*). Mixing at proportions of 7:7:6 yields a good approximation for the composition of sample NZ 560 A, a mixing proportion of 2:11:40 approximates NZ 552. Note, that even at relatively high contributions of subduction related components, no typical negative troughs of Nb and Ta are developed

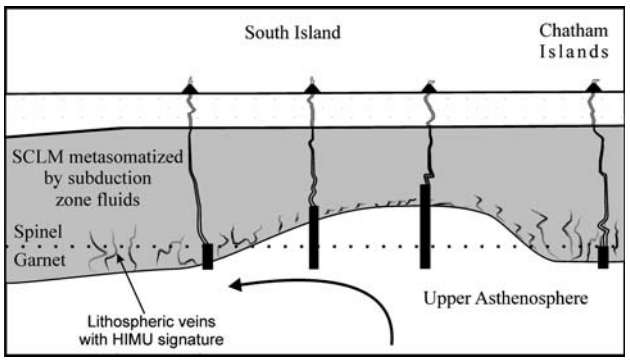

Fig. 10 Schematic sketch illustrating the proposed petrogenetic model for the generation of intraplate magmas on the South Island and the Chatham Islands. *Black boxes* represent different polybaric melting columns

sional stress field (Fig. 11). For the South Island, two tectonic periods can be distinguished. The oldest sample (NZ 555, ~34 Ma) was derived from relatively shallow depth (Fig. 10) and erupted during a period of oblique extension (e.g. Sutherland 1999a). The important role of both, lithospheric wall-rock and an asthenospheric component, is evident from a strongly diluted ''HIMU-like'' trace element pattern and a distinct Pb and Sr isotope composition. Younger samples from the South Island all erupted during a period of oblique transpression with major dextral strike slip motion and lithospheric shearing (<23 Ma; e.g. King 2000). The youngest sample (NZ 552, ~2.52 Ma) erupted when compression had culminated (e.g. King 2000). With decreasing age, the inferred lithospheric thickness and affinities to HIMU decrease while the influence of the lithospheric wall-rock assemblage and the asthenosphere increase. The dimishing lithospheric thickness with time probably reflects transtension and shearing in the lithospheric mantle due to ongoing

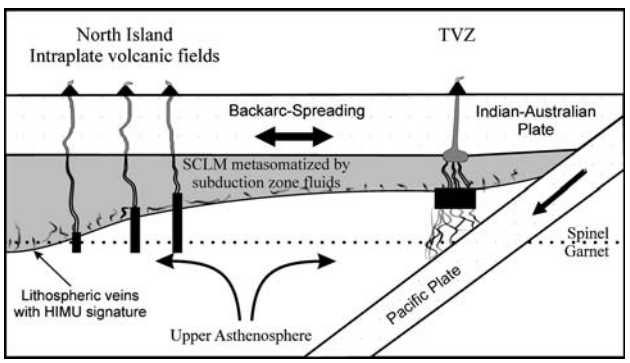

Fig. 11 Schematic sketch illustrating the proposed petrogenetic model for the generation of intraplate magmas on the North Island. *Black boxes* represent different polybaric melting columns. TVZ is ''Taupo Volcanic Zone'', the active arc chain on the North Island

strike slip motion (e.g. Vaughan and Scarrow 2003). In support for such a model, Molnar et al. (1999) and Stern et al. (2000) argued for the presence of a cold slab of lithospheric material sinking beneath the plate boundary, potentially causing extension in the adjacent lithospheric mantle. Furthermore, as previously shown by Little et al. (2002), the deformation of the lithospheric mantle beneath New Zealand extends well into the area beneath the Cenozoic volcanic fields and can even be observed in mantle xenoliths (Duclos et al. 2005). A further thermal erosion of the lithospheric mantle may have been triggered by a delamination induced ascent of asthenospheric material (Tanton and Hager 2000) and increased convection due to an evolving topography at the base of the SCLM (e.g. King and Anderson 1998). Thus, the observed relationship between melting depth and isotope signatures can be explained by a decrease in lithospheric thickness that was triggered by continuous shearing of the SCLM along the New Zealand plate boundary.

As proposed earlier (e.g. Panter et al. 2000; Storey et al. 1999; Weaver et al. 1994) the infiltration of the lithospheric mantle by ''HIMU-like'' melts can possibly be related to the involvement of a HIMU-type plume in the late Cretaceous breakup of East Gondwana. Although a detailed discussion of the origin of ''HIMU-like'' signatures in the SW Pacific would be beyond the scope of this paper, some new contributions can be made on the basis of our New Zealand data. In recent models (Finn et al. 2005; Panter et al. 2006), the SW Pacific HIMU signatures have been explained with metasomatism by subduction components following models of chromatographic metasomatism (e.g. Ionov and Hofmann 1995; Stein et al. 1997) with a subsequent dehydration. In these models, trace element enriched fluids released from the subducting slab precipitate vein assemblages containing amphibole and phlogopite at the cold base of the mantle wedge. Subsequently, due to buoyancy controlled convection, this material gets transported to the base of the lithospheric mantle, where according to Finn et al. (2005) and Panter et al. (2006) it partly dehydrates, creating elevated U-Th/Pb and low Rb/Sr that can evolve to ''HIMU-like'' signatures if isolated over geological time spans. Although this model is appealing because of its link to the regional geologic history, it may not be consistent with the observed isotope compositions for two reasons. First, the extremely elevated $^{207}Pb/^{204}Pb$ and $^{206}Pb/^{204}Pb$ of ''HIMU-like'' samples cannot be explained by a relatively young (Palaeozoic to Mesozoic) formation age from a MORB-like isotopic starting composition. The high $^{207}Pb/^{204}Pb$ would require an earlier (Proterozoic)

formation age. Secondly the distinct ''HIMU-like'' Hf-Nd isotope compositions plotting off the mantle array towards lower εHf (Fig. 5) is inconsistent with a derivation from subduction zone fluids.

The high Zr/Hf in the New Zealand rocks (up to ca. 55), displaying a positive trend with $^{206}Pb/^{204}Pb$ for the South Island data and a negative trend with $^{87}Sr/^{86}Sr$ (not shown), lend further support to a model, where the enriched lithospheric vein component is derived from a HIMU-type source. Similar to our observation for the South Island subset, elevated Zr/Hf in OIBs and intraplate volcanic rocks have been reported (e.g. David et al. 2000; Dupuy et al. 1992) and Geldmacher et al. (2006) also reported a positive coupling of Zr/Hf with $^{206}Pb/^{204}Pb$. The elevated Zr/Hf are unusual for mafic rocks, where Zr/Hf typically scatter around the chondritic value of 34.2 ± 0.3 (Weyer et al. 2002). Previous explanations of this feature include carbonatitic metasomatism (Dupuy et al. 1992), fractionation by residual clinopyroxene during partial melting (David et al 2000), and melting of an eclogite source (Klemme et al. 2002). Carbonatitic metasomatism can be excluded for our data set because there are no negative troughs of Nb and Ta on mantle normalised multi element diagrams (Fig. 3), a feature that is typical for carbonatitic metasomatism (Ionov et al. 1993). Fractionation by residual clinopyroxene is not capable of generating such highly fractionated Zr/Hf values. Tapping of an eclogite-rich residuum is therefore the most plausible model. This is because Zr is enriched in the residuum relative to Hf by melt extraction in the presence of Ca-rich garnet that is typical for eclogitic assemblages (Green et al. 2000; Klemme et al. 2002; van Westrenen et al. 2001a). Consequently, recycled oceanic crust should display high Zr/Hf, high U/Pb and low Rb/Sr (due to fluid extraction during subduction). Combined evidence from Zr/Hf, $^{206}Pb/^{204}Pb$, and $^{87}Sr/^{86}Sr$ therefore provides additional support for a HIMU-type origin of the lithospheric vein component in the source of the New Zealand magmas. Moreover, the unusually radiogenic εNd for a given εHf in the New Zealand rocks are typical for HIMU (e.g. Stracke et al. 2003) and further corroborate a derivation of this component from recycled oceanic crust. This is because D_{Lu}/D_{Hf} in Ca-rich garnet is ~1.3 and D_{Sm}/D_{Nd} is ~4–7.7, resulting in a larger fractionation of Sm/Nd than Lu/Hf during partial melting (van Westrenen et al. 1999, 2001a, Nd partition coefficients calculated after van Westrenen et al. 2001b). Because of its extremely dehydrated nature (Dixon et al. 2002) melts derived from a HIMU-type mantle do not necessarily display highly elevated Rb/Sr and low U/Pb and are thus supposed to preserve their distinctive isotopic composition even if stored in the lithospheric mantle over geologic time. The evolution of the Hf-Nd systematics in lithospheric veins highly depends on their time of storage (Jung et al. 2005).

Recent studies have shown that radiogenic $^{206}Pb/^{204}Pb$ (<20.5) which usually also have been attributed to ''HIMU-like'' mantle components are also present in FOZO-type mantle domains, i.e. isolated trace element enriched domains in the upper asthenospheric mantle (e.g. Stracke et al. 2005). Hence, some of the less radiogenic $^{206}Pb/^{204}Pb$ signatures of the New Zealand volcanic fields might be explained by tapping of a widespread FOZO-like asthenospheric component. Such a model, however, is clearly inconsistent with the presence of residual hydrous K-rich mineral phases in the magma sources, a feature restricted to the lithospheric mantle. Furthermore, the trend displayed by the South Island subset implies the existence of a more extreme isotopic ''end member'' probably resembling the composition of the Chatham Island samples.

SW Pacific and SE correlations

There are several striking similarities between compositions of intraplate volcanic rocks in Zealandia (e.g. Cook 2002; Cook et al. 2005; Huang et al. 1997, 2000; Panter et al. 2006) and those of intraplate volcanic rocks elsewhere in the SW Pacific realm (e.g. Lanyon et al. 1993; Storey et al. 1999; Rocholl et al. 1995; Zhang et al. 2001; O'Reilly and Zhang 1995; Hart et al. 1995, 1997; Hole et al. 1993; Panter et al. 2000; Finn et al. 2005). These similarities include trace element signatures similar to HIMU-OIB as well as highly radiogenic $^{206}Pb/^{204}Pb$. As reported previously (e.g. Finn et al. 2005; Weaver et al. 1994), the strongest affinities to HIMU occur in areas that were juxtaposed to each other prior to the breakup of East Gondwana (i.e. Marie Byrd Land, South Island, Chatham Rise, Campbell Plateau). However, in most cases ''HIMU-like'' components alone are insufficient to explain the observed compositional variations and additional enriched mantle components were proposed. A variety of models were suggested for the origin of these components and their location in the mantle (e.g. Cook 2002; Zhang et al. 2001; Panter et al. 2000; Rocholl et al. 1995; Hart et al. 1995, 1997; Hole et al. 1993). Most models either invoke a distinct spatial distribution, mostly with melting depth (e.g. Rocholl et al. 1995; Huang et al. 2000, Hole et al. 1993; Zhang et al. 2001, Hart et al. 1997). A similar relationship between tectonic setting and magma compositions has been reported for parts of Antarctica (e.g. Hart et al. 1995, 1997; Hole et al. 1993;

Rocholl et al. 1995). Furthermore, hydrous lithospheric mantle appears to be widespred beneath Zealandia and the SW Pacific as suggested by K-anomalies in most intraplate magmas (e.g. Finn et al. 2005; Gamble et al. 1986). It therefore appears plausible, that the lithospheric fragments in former East Gondwana probably share a similar history.

Previous studies on SW Pacific intraplate volcanics frequently argued for the presence of an EM-2-like asthenospheric mantle reservoir in the magma sources (e.g. Hart et al. 1995; Huang et al. 2000; Storey et al. 1999; Zhang et al. 2001). Our model proposing a SCLM modified by subduction components has the advantage to tie the observed signatures to the well-documented geologic record. The model can furthermore explain systematic regional variations of magmas throughout the SW Pacific area. Volcanic fields in East Australia, for example, display less radiogenic $^{206}Pb/^{204}Pb$ and distinctly higher $^{87}Sr/^{86}Sr$ values than volcanic fields in New Zealand and Antarctica. Southeastern Australia was accreted earlier to the Gondwana margin than present day New Zealand and was located in a paleogeographic position further inland from the active Mesozoic continental margin (e.g. Sutherland 1999a). This older history of subduction and a larger distance from the postulated Late Cretaceous Plume can account for a longer period of radiogenic ingrowths at higher Rb/Sr and lower U/Pb ratios and a weaker imprint of HIMU-type melts in the lithospheric mantle beneath East Australia. Collectively, the similarity of the New Zealand rocks to other intraplate volcanic rocks in East Gondwana confirms that old Gondwana-derived lithospheric mantle is present in all source regions (Finn et al. 2005).

Conclusions

A petrogenetic model assuming pooling of polybaric melts from mixed lithospheric and asthenospheric source regions can explain the compositions of mafic volcanic rocks from intraplate volcanic fields throughout Zealandia. Three compositional end members are distinguished: (1) The hydrous SCLM that was metasomatised by subduction components during the Palaeozoic to Cretaceous; (2) frozen ''fossil'' melt veins within the SCLM that possibly originate from a Cretaceous HIMU-type plume; (3) an upper asthenospheric component similar to the depleted mantle.

The different tectonic regimes present in New Zealand result in variations of lithospheric thickness, lithospheric strain, and asthenospheric heat flow. Beneath the North Island, the asthenospheric component dominates due to higher rates of extension, resulting in more diluted lithospheric signatures. For the South Island, an increase in the portion of HIMU-type component is observed with increasing average melting depth. The higher average melting depth reflects a larger lithospheric thickness. Shallower melting depths are coupled to greater degrees of melting and a thinner lithosphere. The decrease in melting depth beneath the South Island is attributed to pervasive shearing and possible delamination of the SCLM. Temporal and spatial variations in the New Zealand rocks argue against the presence of active mantle plumes. Given the regional similarities, in particular the evidence for the widespread presence of hydrous lithospheric mantle, our proposed model may also be applicable to other volcanic fields in former East Gondwana. In a general context, our results emphasize the importance of the SCLM as a distinct geochemical reservoir that significantly contributes to the trace element and isotope inventory of intraplate magmas. Certain domains in the SCLM may preserve geochemical signatures of previous tectonomagmatic events. Regional structural dynamics appear to play a significant role in controlling the properties of continental intraplate volcanism.

Acknowledgments Dieter Garbe-Schönberg from Universität Kiel and Radegund Hoffbauer and Beate Trenkle from Universität Bonn are thanked for ICP-MS analyses and XRF analyses, respectively. We thank Heidi Baier from Universität Münster for lab support. Tony Reay and Bruce Hayward provided useful information and access to some field areas. Mark Rattenbury, Dave Heron, John Simes and Neville Orr from IGNS Lower Hutt provided useful information, maps, and kind support during sample preparation. Oliver Nebel and Yona Nebel-Jacobsen are thanked for assistance during fieldwork. Erik Scherer contributed valuable comments. We thank John Gamble and Andreas Stracke for thoughtful reviews that greatly helped to improve the manuscript and Jochen Hoefs for editorial handling. Andreas Stracke is thanked for an updated version of his isotope database for oceanic basalts.

References

Adams CJ (1981) Migration of Late Cenozoic volcanism in the South Island of New Zealand and the Campbell Plateau. Nature 294(5837):153–155

Asimow PD, Langmuir CH (2003) The importance of water to oceanic mantle melting regimes. Nature 421(6925):815–820

Asimow PD, Dixon JE, Langmuir CH (2004) A hydrous melting and fractionation model for mid-ocean ridge basalts: application to the mid-atlantic ridge near the Azores. Geochemistry Geophysics Geosystems 5

Baker JA, Gamble JA, Graham IJ (1994) The age, geology, and geochemistry of the Tapuaenuku Igneous Complex, Marlborough, New-Zealand. NZ J Geol Geophys 37(3):249–268

Blichert-Toft J, Albarède F (1997) The Lu-Hf isotope geochemistry of chondrites and the evolution of the mantle-crust system. Earth Planet Sci Lett 148(1–2):243–258

Bogaard PJF, Wörner G (2003) Petrogenesis of basanitic to tholeiitic volcanic rocks from the Miocene Vogelsberg, Central Germany. J Petrol 44(3):569–602

Boynton WV (1984) Cosmochemistry of the rare earth elements; meteorite studies. In: Henderson P (ed) Rare earth element geochemistry. Elsevier Sci. Publ. Co., Amsterdam, pp 63–114

Briggs RM, McDonough WF (1990) Contemporaneous convergent margin and intraplate magmatism, North Island, New-Zealand. J Petrol 31(4):813–851

Briggs RM, Itaya T, Lowe DJ, Keane AJ (1989) Ages of the Pliocene Pleistocene Alexandra and Ngatutura Volcanics, Western North-Island, New-Zealand, and some geological implications. NZ J Geol Geophys 32(4):417–427

Briggs RM, Okada T, Itaya T, Shibuya H, Smith IEM (1994) K-Ar Ages, Paleomagnetism, and geochemistry of the South Auckland Volcanic Field, North-Island, New-Zealand. NZ J Geol Geophys 37(2):143–153

Chauvel C, Blichert-Toft J (2001) A hafnium isotope and trace element perspective on melting of the depleted mantle. Earth Planet Sci Lett 190(3–4):137–151

Class C, Goldstein SL (1997) Plume-lithosphere interactions in the ocean basins: constraints from the source mineralogy. Earth Planet Sci Lett 150(3–4):245–260

Cook C (2002) Petrogenesis and evolution of alkalic basaltic magmas in a continental intraplate setting: The South Auckland volcanic field, New Zealand. University of Waikato, Hamilton

Cook C, Briggs RM, Smith IEM, Maas R (2005) Petrology and geochemistry of intraplate basalts in the South Auckland volcanic field, New Zealand: evidence for two coeval magma suites from distinct sources. J Petrol 46(3):473–503

Dasgupta R, Hirschmann MM, Stalker K (2006) Immiscible transition from carbonate-rich to silicate-rich melts in the 3 GPa melting interval of eclogite plus CO_2 and genesis of silica-undersaturated ocean island lavas. J Petrol 47(4):647–671

David K, Schiano P, Allegre CJ (2000) Assessment of the Zr/Hf fractionation in oceanic basalts and continental materials during petrogenetic processes. Earth Planet Sci Lett 178(3–4):285–301

Dixon JE, Leist L, Langmuir C, Schilling J-G (2002) Recycled dehydrated lithosphere observed in plume-influenced mid-ocean-ridge basalt. Nature 420(6914):385

Duclos M, Savage MK, Tommasi A, Gledhill KR (2005) Mantle tectonics beneath New Zealand inferred from SKS splitting and petrophysics. Geophys J Int 163(2):760–774

Dupuy C, Liotard JM, Dostal J (1992) Zr/Hf fractionation in intraplate basaltic rocks - carbonate metasomatism in the mantle source. Geochimica et Cosmochimica Acta 56(6):2417–2423

Eagles G, Gohl K, Larter RD (2004) High-resolution animated tectonic reconstruction of the South Pacific and West Antarctic margin. Geochemistry Geophysics Geosystems 5: paper no. DOI:10.1029/2003GC000657

Ellam RM, Cox KG (1989) A Proterozoic lithospheric source for Karoo Magmatism - evidence from the Nuanetsi Picrites. Earth Planet Sci Lett 92(2):207–218

Ellam RM, Cox KG (1991) An interpretation of Karoo Picrite Basalts in terms of interaction between asthenospheric magmas and the mantle lithosphere. Earth Planet Sci Lett 105(1–3):330–342

Falloon TJ, Green DH (1990) Solidus of carbonated fertile peridotite under fluid-saturated conditions. Geology 18(3):195–199

Finn CA, Müller RD, Panter KS (2005) A Cenozoic diffuse alkaline magmatic province (DAMP) in the southwest Pacific without rift or plume origin. Geochemistry Geophysics Geosystems 6: paper no. DOI:10.1029/2004GC000723

Foley S (1991) High-Pressure stability of the fluor-endmembers and hydroxy-endmembers of Pargasite and K-Richterite. Geochimica et Cosmochimica Acta 55(9):2689–2694

Foley S (1992) Vein-Plus-Wall-Rock melting mechanisms in the lithosphere and the origin of potassic alkaline magmas. Lithos 28(3–6):435–453

Gallagher K, Hawkesworth C (1992) Dehydration melting and the generation of Continental Flood Basalts. Nature 358(6381):57–59

Gamble JA, Morris PA, Adams CJ (1986) The geology, petrology and geochemistry of Cenozoic volcanic rocks from the Campbell plateau and Chatham rise. In: Smith IEM (ed) Late Cenozoic volcanism in New Zealand. The Royal Society of New Zealand Bulletin 23:344–365

Geldmacher J, Hoernle K, Klugel A, van den Bogaard P, Duggen S (2006) A geochemical transect across a heterogeneous mantle upwelling: implications for the evolution of the Madeira hotspot in space and time. Lithos 90(1–2):131–144

Govindaraju K (1994) 1994 Compilation of working values and sample description for 383 geostandards. Geostandards Newsletter *18*, Special Issue, 1–158

Graham DW (2002) Noble gas isotope geochemistry of mid-ocean ridge and ocean island basalts: characterization of mantle source reservoirs. In: Noble gases in geochemistry and cosmochemistry. 47:247–317

Green DH (1973) Experimental melting studies on a model upper mantle composition at high pressure under water-saturated and water-undersaturated conditions. Earth Planet Sci Lett 19(1):37–53

Green TH, Blundy JD, Adam J, Yaxley GM (2000) SIMS determination of trace element partition coefficients between garnet, clinopyroxene and hydrous basaltic liquids at 2–7.5 GPa and 1080–1200°C. Lithos 53(3–4):165–187

Grégoire M, Bell DR, Le Roex AP (2002) Trace element geochemistry of phlogopite-rich mafic mantle xenoliths: their classification and their relationship to phlogopite-bearing peridotites and kimberlites revisited. Contrib Mineral Petrol 142(5):603–625

Grindley GW, Adams CJD, Lumb JT, Watters WA (1977) Paleomagnetism, K-Ar dating and tectonic interpretation of Upper Cretaceous and Cenozoic volcanic rocks of Chatham Islands, New-Zealand - With an appendix dating of Pliocene volcanic rocks. NZ J Geol Geophys 20(3):425–467

Halliday A, Lee DC, Tommasini S, Davies GR, Paslick CR, Fitton JG, James DE (1995) Incompatible trace-elements in OIB and MORB and source enrichment in the sub-oceanic mantle. Earth Planet Sci Lett 133(3–4):379–395

Handler MR, Wysoczanski RJ, Gamble JA (2003) Proterozoic lithosphere in Marie Byrd Land, West Antarctica: Re-Os systematics of spinel peridotite xenoliths. Chem Geol 196(1–4):131–145

Handler MR, Bennett VC, Carlson RW (2005) Nd, Sr and Os isotope systematics in young, fertile spinel peridotite xenoliths from northern Queensland, Australia: a unique view of depleted MORB mantle? Geochimica Et Cosmochimica Acta 69(24):5747–5763

Hart SR, Dunn T (1993) Experimental Cpx/Melt partitioning of 24 trace-elements. Contrib Mineral Petrol 113(1):1–8

Hart SR, Blusztajn J, Craddock C (1995) Cenozoic volcanism in Antarctica - Jones mountains and Peter-I Island. Geochimica et Cosmochimica Acta 59(16):3379–3388

Hart SR, Blusztajn J, LeMasurier WE, Rex DC (1997) Hobbs Coast Cenozoic volcanism: implications for the West Antarctic rift system. Chem Geol 139(1–4):223–248

Hawkesworth CJ, Gallagher K (1993) Mantle hotspots, plumes and regional tectonics as causes of intraplate magmatism. Terra Nova 5(6):552–559

Hawkesworth CJ, Kempton PD, Rogers NW, Ellam RM, VanCalsteren PW (1990) Continental mantle lithosphere, and shallow level enrichment processes in the Earths Mantle. Earth Planet Sci Lett 96(3–4):256–268

Heinrichs H, Hermann AG (1990) Praktikum der analytischen Geochemie. Springer, Heidelberg, pp 667

Heming RF (1980a) Patterns of quaternary basaltic volcanism in the northern North-Island, New-Zealand. NZ J Geol Geophys 23(3):335–344

Heming RF (1980b) Petrology and geochemistry of quaternary basalts from Northland, New-Zealand. J Volcanol Geothermal Res 8(1):23–44

Heming RF, Barnet PR (1986) The petrology and petrochemistry of the Auckland Volcanic Field. In: Smith IEM (ed) Late cenozoic volcanism in New Zealand. The Royal Society of New Zealand Bulletin 23:64–75

Herzberg C (1995) Generation of plume magmas through time - an experimental perspective. Chem Geol 126(1):1–16

Hieronymus CF, Bercovici D (1999) Discrete alternating hotspot islands formed by interaction of magma transport and lithospheric flexure. Nature 397(6720):604–607

Hieronymus CF, Bercovici D (2000) Non-hotspot formation of volcanic chains: control of tectonic and flexural stresses on magma transport. Earth Planet Sci Lett 181(4):539–554

Hirschmann MM, Kogiso T, Baker MB, Stolper EM (2003) Alkalic magmas generated by partial melting of garnet pyroxenite. Geol 31(6):481–484

Hodder APW (1984) Late Cenozoic rift development and intraplate volcanism in Northern New-Zealand inferred from geochemical discrimination diagrams. Tectonophysics 101(3–4):293–318

Hofmann AW (1988) Chemical differentiation of the Earth: the relationship between mantle, continental crust, and oceanic crust. Earth Planet Sci Lett 90(3):297–314

Hofmann AW (1997) Mantle geochemistry: the message from oceanic volcanism. Nature 385(6613):219–229

Hoke L, Poreda R, Reay A, Weaver SD (2000) The subcontinental mantle beneath southern New Zealand, characterised by helium isotopes in intraplate basalts and gas-rich springs. Geochimica et Cosmochimica Acta 64(14):2489–2507

Hole MJ, Kempton PD, Millar IL (1993) Trace-Element and isotopic characteristics of small-degree melts of the asthenosphere - evidence from the alkalic basalts of the Antarctic Peninsula. Chem Geol 109(1–4):51–68

Huang Y, Hawkesworth C, van Calsteren P, Smith I, Black P (1997) Melt generation models for the Auckland volcanic field, New Zealand: constraints from U-Th isotopes. Earth Planet Sci Lett 149(1–4):67

Huang Y, Hawkesworth C, Smith I, van Calsteren P, Black P (2000) Geochemistry of late Cenozoic basaltic volcanism in Northland and Coromandel, New Zealand: implications for mantle enrichment processes. Chem Geol 164(3–4):219

Ionov DA, Hofmann AW (1995) Nb-Ta-rich mantle amphiboles and micas - implications for subduction-related metasomatic trace-element fractionations. Earth Planet Sci Lett 131(3–4):341–356

Ionov DA, Dupuy C, O'Reilly SY, Kopylova MG, Genshaft YS (1993) Carbonated peridotite xenoliths from Spitsbergen - implications for trace-element signature of mantle carbonate metasomatism. Earth Planet Sci Lett 119(3):283–297

Ionov DA, Griffin WL, O'Reilly SY (1997) Volatile-bearing minerals and lithophile trace elements in the upper mantle. Chem Geol 141(3–4):153–184

Ionov DA, Shirey SB, Weis D, Brugmann G (2006) Os-Hf-Sr-Nd isotope and PGE systematics of spinel peridotite xenoliths from Tok, SE Siberian craton: effects of pervasive metasomatism in shallow refractory mantle. Earth Planet Sci Lett 241(1–2):47–64

Jacobsen SB, Wasserburg GJ (1980) Sm-Nd isotopic evolution of chondrites. Earth Planet Sci Lett 50(1):139–155

Jung S, Pfänder JA, Brügmann G, Stracke A (2005) Sources of primitive alkaline volcanic rocks from the Central European Volcanic Province (Rhön, Germany) inferred from Hf, Os and Pb isotopes. Contrib Mineral Petrol 150(5):546–559

Kamp PJJ (1986) Late Cretaceous-Cenozoic tectonic development of the Southwest Pacific region. Tectonophysics 121(2–4):225–251

King PR (2000) Tectonic reconstructions of New Zealand: 40 Ma to the present. NZ J Geol Geophys 43(4):611–638

King SD, Anderson DL (1998) Edge-driven convection. Earth Planet Sci Lett 160(3–4):289–296

Klemme S, Blundy JD, Wood BJ (2002) Experimental constraints on major and trace element partitioning during partial melting of eclogite. Geochimica et Cosmochimica Acta 66(17):3109–3123

Kogiso T, Tatsumi Y, Nakano S (1997) Trace element transport during dehydration processes in the subducted oceanic crust.1. Experiments and implications for the origin of ocean island basalts. Earth Planet Sci Lett 148(1–2):193–205

Kogiso T, Hirschmann MM, Frost DJ (2003) High-pressure partial melting of garnet pyroxenite: possible mafic lithologies in the source of ocean island basalts. Earth Planet Sci Lett 216(4):603–617

Kogiso T, Hirschmann MM, Pertermann M (2004) High-pressure partial melting of mafic lithologies in the mantle. J Petrol 45(12):2407–2422

Langmuir CH, Klein EM, T. P (1992) Petrological systematics of mid-ocean ridge basalts: constraints on melt generation beneath ocean ridges. In: Morgan JP, Blackman DK, Sinton JM (eds) Mantle flow and melt generation at mid-ocean ridges. American Geophysical Union, Washington, DC, Geophysical Monograph 71:183–280

Lanyon R, Varne R, Crawford AJ (1993) Tasmanian tertiary basalts, the Balleny Plume, and opening of the Tasman Sea (Southwest Pacific-Ocean). Geology 21(6):555–558

LaTourrette T, Hervig RL, Holloway JR (1995) Trace-element partitioning between amphibole, phlogopite, and basanite melt. Earth Planet Sci Lett 135(1–4):13–30

Le Maître RW, Bateman P, Dudek A, Keller J, Lameyre J, Le Bas MJ, Sabine PA, Schmid R, Sorensen H, Streckeisen A, Woolley AR, Zanettin B (1989) A classification of igneous rocks and glossary of terms: recommendations of the international union of geological sciences subcommission on the systematics of igneous rocks. Blackwell Scientific, Oxford

Le Roex AP, Späth A, Zartman RE (2001) Lithospheric thickness beneath the southern Kenya Rift: implications from basalt geochemistry. Contrib Mineral Petrol 142(1):89–106

Lebrun JF, Lamarche G, Collot JY, Delteil J (2000) Abrupt strike-slip fault to subduction transition: The Alpine Fault-

Puysegur Trench connection, New Zealand. Tectonics 19(4):688–706
Li ZX, Powell CM (2001) An outline of the palaeogeographic evolution of the Australasian region since the beginning of the Neoproterozoic. Earth Sci Rev 53(3–4):237–277
Little TA, Savage MK, Tikoff B (2002) Relationship between crustal finite strain and seismic anisotropy in the mantle, Pacific-Australia plate boundary zone, South Island, New Zealand. Geophys J Int 151(1):106–116
Lugmair GW, Marti K (1978) Lunar Initial Nd-143-Nd-144 - Differential Evolution Of Lunar Crust And Mantle. Earth Planet Sci Lett 39(3):349–357
Luyéndyk BP (1995) Hypothesis for Cretaceous rifting of east Gondwana caused by subducted slab capture. Geology 23(4):373–376
Manhes G, Allègre CJ, Provost A (1984) U-Th-Pb systematics of the eucrite ''Juvinas'': Precise age determination and evidence for exotic lead. Geochimica et Cosmochimica Acta 48(11):2247–2264
Mattinson JM (1986) Geochronology of high-pressure-low temperature Fanciscan metabasites: a new approach using the U-Pb system. Geol Soc Am Memoire 164:95–105
McBride JS, Lambert DD, Greig A, Nicholls IA (1996) Multistage evolution of Australian subcontinental mantle: Re-Os isotopic constraints from Victorian mantle xenoliths. Geology 24(7):631–634
McDonough WF, Sun SS (1995) The composition of the Earth. Chem Geol 120(3–4):223–253
McKenzie D (1989) Some remarks on the movement of small melt fractions in the mantle. Earth Planet Sci Lett 95(1–2):53–72
McKenzie D, Bickle MJ (1988) The volume and composition of melt generated by extension of the lithosphere. J Petrol 29(3):625–679
McKenzie D, Jackson J, Priestley K (2005) Thermal structure of oceanic and continental lithosphere. Earth Planet Sci Lett 233(3–4):337–349
Mitchell RH (1995) Melting experiments on a Sanidine Phlogopite Lamproite at 4–7 GPa and their bearing on the sources of Lamproitic Magmas. J Petrol 36(5):1455–1474
Molnar P, Anderson HJ, Audoine E, Eberhart-Phillips D, Gledhill KR, Klosko ER, McEvilly TV, Okaya D, Savage MK, Stern T, Wu FT (1999) Continous deformation versus faulting through the continental lithosphere of New Zealand. Science 286(5439):516–519
Mortimer N (2004) New Zealand's geological foundations. Gondwana Res 7(1):261–272
Münker C, Weyer S, Scherer E, Mezger K (2001) Separation of high field strength elements (Nb, Ta, Zr, Hf) and Lu from rock samples for MC-ICPMS measurements. Geochemistry Geophysics Geosystems 2: paper no. 10.1029/2001GC000183\insrsid8857922
Münker C, Pfänder JA, Weyer S, Büchl A, Kleine T, Mezger K (2003) Evolution of planetary cores and the Earth-Moon System from Nb/Ta Systematics. Science 301(5629):84–87
O'Reilly SY, Zhang M (1995) Geochemical characteristics of lava-field basalts from Eastern Australia and inferred sources - connections with the subcontinental lithospheric mantle. Contrib Mineral Petrol 121(2):148–170
Olafsson M, Eggler DH (1983) Phase relations of amphibole, amphibole-carbonate, and phlogopite-carbonate peridotite: petrologic constraints on the asthenosphere. Earth Planet Sci Lett 64(2):305–315
Panter KS, Hart SR, Kyle P, Blusztanjn J, Wilch T (2000) Geochemistry of Late Cenozoic basalts from the Crary Mountains: characterization of mantle sources in Marie Byrd Land, Antarctica. Chem Geol 165(3–4):215–241
Panter KS, Blusztajn J, Hart S, Finn C, Kyle P (2005) A HIMU source in metasomatised continental lithosphere. Geochimica et Cosmochimica Acta 69(10):A97–A97
Panter KS, Blusztajn J, Hart SR, Kyle PR, Esser R, McIntosh WC (2006) The origin of HIMU in the SW Pacific: evidence from intraplate volcanism in Southern New Zealand and Subantarctic Islands. J Petrol 47(9):1673–1704
Patterson DB, Honda M, McDougall I (1994) Noble-Gases in mafic phenocrysts and xenoliths from New-Zealand. Geochimica et Cosmochimica Acta 58(20):4411–4427
Pin C, Joannon S, Bosq C, Le Fevre B, Gauthier PJ (2003) Precise determination of Rb, Sr, Ba, and Pb in geological materials by isotope dilution and ICP-quadrupole mass spectrometry following selective separation of the analytes. J Anal Atomic Spectrometry 18(2):135–141
Plank T, Langmuir CH (1998) The chemical composition of subducting sediment and its consequences for the crust and mantle. Chem Geol 145(3–4):325–394
Rafferty WJ, Heming RF (1979) Quaternary alkalic and subalkalic volcanism in South Auckland, New-Zealand. Contrib Mineral Petrol 71(2):139–150
Reay A, Parkinson D (1997) Adakites from Solander Island, New Zealand. NZ J Geol Geophys 40(2):121–126
Richard P, Shimizu N, Allègre CJ (1976) Nd-143-Nd-146 A aatural tracer - application to oceanic basalts. Earth Planet Sci Lett 31(2):269–278
Rocholl A, Stein M, Molzahn M, Hart SR, Wörner G (1995) Geochemical evolution of rift magmas by progressive tapping of a stratified mantle source beneath the Ross-Sea-Rift, Northern Victoria-Land, Antarctica. Earth Planet Sci Lett 131(3–4):207–224
Rudnick RL, Gao S (2003) The composition of the continental crust. In: Rudnick RL (eds) The crust, treatise on geochemistry. Elsevier-Pergamon, Oxford 3:1–64
Salters VJM, Stracke A (2004) Composition of the depleted mantle. Geochemistry Geophysics Geosystems 5
Scherer EE, Münker C, Rehkämper M, Mezger K (1999) Improved precision of Lu isotope dilution measurements by MC-ICP-MS and application to Lu-Hf geochronology. Eos Suppl. 80(46):1118
Scherer E, Münker C, Mezger K (2001) Calibration of the lutetium-hafnium clock. Science 293(5530):683–687
Schuth S, Rohrbach A, Münker C, Ballhaus C, Garbe-Schönberg D, Qopoto C (2004) Geochemical constraints on the petrogenesis of arc picrites and basalts, New Georgia Group, Solomon Islands. Contrib Mineral Petrol 148(3):288–304
Shaw DM (1970) Trace element fractionation during anatexis. Geochimica et Cosmochimica Acta 34(2):237–243
Smith IEM, Okada T, Itaya T, Black PM (1993) Age relationships and tectonic implications of late Cenozoic basaltic volcanism in Northland, New-Zealand. NZ J Geol Geophys 36(3):385–393
Späth A, Le Roex AP, Opiyo-Akech N (2001) Plume-lithosphere interaction and the origin of continental rift-related alkaline volcanism - the Chyulu Hills Volcanic Province, southern Kenya. J Petrol 42(4):765–787
Spörli KB (1980) New Zealand and oblique-slip margins: tectonic development up to and during the Cainozoic. In: Ballance PF, Reading HG (eds) Sedimentation in oblique-slip mobile zones. International Association of Sedimentologists, Special Publications 4:147–170

Sprung P, Schuth S, Nebel O, Münker C, Hoke L (2005) Intraplate volcanism in New Zealand: asthenospheric versus lithospheric contributions. Eur J Mineral 17(Beiheft):132

Steiger RH, Jäger E (1977) Subcommission on geochronology - convention on use of decay constants in geochronology and cosmochronology. Earth Planet Sci Lett 36(3):359–362

Stein M, Navon O, Kessel R (1997) Chromatographic metasomatism of the Arabian–Nubian lithosphere. Earth Planet Sci Lett 152(1–4):75–91

Steinberger B, Sutherland R, O'Connell RJ (2004) Prediction of Emperor-Hawaii seamount locations from a revised model of global plate motion and mantle flow. Nature 430(6996):167–173

Stern T (1985) A back-arc basin formed within continental lithosphere - the central volcanic region of New Zealand. Tectonophysics 112(1–4):385–409

Stern T, Molnar P, Okaya D, Eberhart-Phillips D (2000) Teleseismic P wave delays and modes of shortening the mantle lithosphere beneath South Island, New Zealand. J Geophys Res-Solid Earth 105(B9):21615–21631

Storey BC, Leat PT, Weaver SD, Pankhurst RJ, Bradshaw JD, Kelley S (1999) Mantle plumes and Antarctica-New Zealand rifting: evidence from mid-Cretaceous mafic dykes. J Geol Soc 156:659–671

Stracke A, Bizimis M, Salters VJM (2003) Recycling oceanic crust: quantitative constraints. Geochemistry Geophysics Geosystems 4 (3): paper no. DOI 10.1029/2001GC000223

Stracke A, Hofmann AW, Hart SR (2005) FOZO, HIMU, and the rest of the mantle zoo. Geochemistry Geophysics Geosystems 6: paper no. doi:10.1029/2004GC000824

Sutherland R (1995) The Australia-Pacific boundary and Cenozoic plate motions in the SW Pacific - some constraints from Geosat Data. Tectonics 14(4):819–831

Sutherland R (1999a) Basement geology and tectonic development of the greater New Zealand region: an interpretation from regional magnetic data. Tectonophysics 308(3):341–362

Sutherland R (1999b) Cenozoic bending of New Zealand basement terranes and Alpine Fault displacement: a brief review. NZ J Geol Geophys 42(2):295–301

Sutherland R, Davey F, Beavan J (2000) Plate boundary deformation in South Island, New Zealand, is related to inherited lithospheric structure. Earth Planet Sci Lett 177(3-4):141–151

Tanton LTE, Hager BH (2000) Melt intrusion as a trigger for lithospheric foundering and the eruption of the Siberian flood basalts. Geophys Res Lett 27(23):3937–3940

Taylor SR, McLennan SM (1985) The Continental Crust: Its composition and evolution. Blackwell Science, Oxford

Tilton GR (1973) Isotopic lead ages of chondritic meteorites. Earth Planet Sci Lett 19(3):321

Todt W, Cliff RA, Hanser A, Hofmann AW (1996) $^{202}Pb + {}^{205}Pb$ double spike for lead isotopic analyses. In: A. B, S. H (eds) Earth processes: reading the isotopic code. Geophysical Monograph 95

Turcotte DL, Emerman SH (1983) Mechanisms of active and passive rifting. Tectonophysics 94(1–4):39–5

Vaughan APM, Scarrow JH (2003) K-rich mantle metasomatism control of localization and initiation of lithospheric strike-slip faulting. Terra Nova 15(3):163–169

Vervoort JD, Patchett JP, Blichert-Toft J, Albarède F (1999) Relationships between Lu-Hf and Sm-Nd isotopic systems in the global sedimentary system. Earth Planet Sci Lett 168:79–99

Waight TE, Weaver SD, Muir RJ (1998) Mid-Cretaceous granitic magmatism during the transition from subduction to extension in southern New Zealand: a chemical and tectonic synthesis. Lithos 45(1–4):469–482

Wallace ME, Green DH (1991) The effect of bulk rock composition on the stability of amphibole in the upper mantle - implications for solidus positions and mantle metasomatism. Mineral Petrol 44(1–2):1–19

Walter MJ (1998) Melting of garnet peridotite and the origin of komatiite and depleted lithosphere. J Petrol 39(1):29–60

Wasserburg GJ, Jacobsen SB, Depaolo DJ, McCulloch MT, Wen T (1981) Precise determination of Sm/Nd ratios, Sm and Nd isotopic abundances in standard solutions. Geochimica et Cosmochimica Acta 45(12):2311–2323

Weaver SD, Smith IEM (1989) New Zealand intraplate volcanism. In: Johnson RW, Knutsen J, Taylor SR (eds) Intraplate volcanism in Eastern Australia and New Zealand. Cambridge University Press, Cambridge, pp 157–188

Weaver SD, Storey B, Pankhurst RJ, Mukasa SB, Divenere VJ, Bradshaw JD (1994) Antarctica New-Zealand rifting and Marie-Byrd-Land lithospheric magmatism linked to ridge subduction and mantle plume activity. Geology 22(9):811–814

Weissel JK, Hayes DE (1977) Evolution of Tasman Sea reappraised. Earth Planet Sci Lett 36(1):77–84

Weissel JK, Hayes DE, Herron EM (1977) Plate tectonics synthesis - displacements between Australia, New-Zealand, and Antarctica since Late Cretaceous. Marine Geol 25(1–3):231–277

van Westrenen W, Blundy JD, Wood BJ (1999) Crystal-chemical controls on trace element partitioning between garnet and anhydrous silicate melt. Am Mineralogist 84:838–847

van Westrenen W, Blundy JD, Wood BJ (2001a) High field strength element/rare earth element fractionation during partial melting in the presence of garnet: implications for identification of mantle heterogeneities. Geochemistry Geophysics Geosystems 2:art. no.-2000GC000133

van Westrenen W, Wood BJ, Blundy JD (2001b) A predictive thermodynamic model of garnet-melt trace element partitioning. Contrib Mineral Petrol 142:219–234

Weyer S, Münker C, Rehkämper M, Mezger K (2002) Determination of ultra-low Nb, Ta. Zr and Hf concentrations and the chondritic Zr/Hf and Nb/Ta ratios by isotope dilution analyses with multiple collector ICP-MS. Chem Geol 187(3–4):295–313

White R, McKenzie D (1989) Magmatism at rift zones - the generation of volcanic continental margins and Flood Basalts. J Geophys Res-Solid Earth Planets 94(B6):7685–7729

Wilson M, Rosenbaum JM, Dunworth EA (1995) Melilitites - partial melts of the thermal-boundary-layer. Contrib Mineral Petrol 119(2–3):181–196

Wood BJ, Blundy JAD (2002) The effect of H2O on crystal-melt partitioning of trace elements. Geochimica et Cosmochimica Acta 66(20):3647–3656

Workman RK, Hart SR (2005) Major and trace element composition of the depleted MORB mantle (DMM). Earth Planet Sci Lett 231(1–2):53–72

Zhang M, Stephenson PJ, O'Reilly SY, McCulloch MT, Norman M (2001) Petrogenesis and geodynamic implications of late Cenozoic basalts in North Queensland, Australia: Trace-element and Sr-Nd-Pb isotope evidence. J Petrol 42(4):685–719

Zindler A, Hart S (1986) Chemical Geodynamics. Ann Rev Earth Planet Sci 14:493–571